Ice algae resource utilization by benthic macro- and megafaunal communities on the Pacific Arctic shelf determined through lipid biomarker analysis

Chelsea Wegner Koch[1*], Lee W. Cooper[1], Jacqueline M. Grebmeier[1], Karen Frey[2], and Thomas A. Brown[3]

[1] Chesapeake Biological Laboratory, University of Maryland Center for Environmental Science, Solomons, MD 20688, USA

[2] Graduate School of Geography, Clark University, Worcester, MA 01610, USA

[3] Scottish Association for Marine Science, Oban PA37 1QA, United Kingdom

[*] Corresponding author: cwegner@umces.edu

Abstract

We studied ice algae utilization by benthic fauna from the northern Bering and Chukchi Seas using highly branched isoprenoid (HBI) biomarkers. We assessed whether various food acquisition strategies influence the observed HBI signatures. The proportion of phytoplankton to ice algae-sourced HBIs was determined through the H-Print approach that is presumed to reflect the percentage of sea ice organic carbon (iPOC) incorporated into tissues, relative to phytoplankton organic carbon. Cluster analysis separated three groups based on location and feeding strategy that were significantly influenced by annual sea ice persistence. Ice algae utilization was most significant in the northeast Chukchi Sea, where seasonal sea ice was present the longest. General feeding strategy was determined to be a significant factor in the degree of ice algae utilization. Predominant deposit feeders (both surface and subsurface) used more ice algae relative to suspension feeders. Organic carbon incorporated by predominant suspension feeders was primarily phytoplankton-based. The vast majority of all organisms sampled (~90%) incorporated a measureable quantity of iPOC. Sipunculids and brittle stars had the highest relative dependence on ice algae, while other taxa displayed plastic dietary responses, including the suspension/surface deposit feeder *Macoma calcarea*. This study indicates that ice algae are widely utilized in Pacific Arctic benthic food webs, but most benthic organisms displayed flexibility in consuming the available food sources. The elevated utilization of ice algae by deposit feeders may prove to be a disadvantage for these organisms if they cannot adapt to the on-going decline of iPOC as seasonal sea ice declines.

1. Introduction

Microalgal primary production on the Pacific Arctic continental shelves is partitioned between ice-associated (sympagic) and pelagic diatoms, and depends on seasonal ice cover dynamics, nutrient availability and water column stratification (Hill et al. 2018, Selz et al. 2018). Strong sympagic-pelagic-benthic coupling has sustained rich benthic ecosystems on this shallow shelf system (Iken et al. 2010, Dunton et al. 2014, Grebmeier et al. 2015). However, declining sea ice cover and persistence along with changes in the timing of the sea ice cycle are likely to disrupt this ecosystem structure (Grebmeier et al. 2006a, Leu et al. 2011, Kędra et al. 2015, Moore et al. 2018). Sea ice has declined overall in the Arctic with pronounced losses in the Bering and Chukchi Seas (Serreze & Meier 2018). The winter of 2017-18 marked the record low maximum sea ice extent for the northern Bering Sea, reaching only 46% (411,500 km^2) of the 1979-2016 mean maximum extent (Thoman et al. 2020). These were levels that were not previously predicted to occur until the 2030s (Stabeno & Bell 2019).

With the increasing open water season for the Pacific Arctic, there are a number of possible outcomes that will impact trophic stability and function as a result of changes in the timing, quality and quantity of the basal food source (Moore & Stabeno 2015). Lower trophic level consumers coordinate life cycles (i.e. spawning, growth, foraging) with the early spring bloom containing sympagic microalgae, where a mismatch in timing could be detrimental to the food web (Søreide et al. 2010, Leu et al. 2011). Ice algae are a high-value food source because of its high polyunsaturated fatty acid composition (Falk-Petersen et al. 1998, McMahon et al. 2006, Søreide et al. 2010, Wang et al. 2014) and high sinking rates (Legendre et al. 1992, Riedel et al. 2006) relative to phytoplankton. Although overall primary production is predicted to increase in the Arctic with global warming (Arrigo 2015, Lewis et al. 2020), it would likely coincide with an

increasing proportion of small pelagic algae with a lower sinking potential (Li et al. 2009) and a decrease in sympagic productivity.

As a result of these changes in primary production, the organic carbon flow in the Pacific Arctic is hypothesized to increase through pelagic trophic chains to the detriment of the benthic ones, which will have a large impact on the whole food web in terms of both quality and standing stock (Kędra et al. 2015, Moore & Stabeno 2015). The shift to a pelagic-dominated food web, together with access to ice-free waters are likely to lead to population increases in foraging pelagic fish, along with water column feeding whales and seabirds (Moore & Huntington 2008, Kędra et al. 2015). As a result, there are expected to be reductions and redistributions of benthic populations that serve as the prey base for higher trophic predators including walruses, bearded seals, spectacled eiders, and gray whales (Grebmeier et al. 2006b, Moore & Huntington 2008, Jay et al. 2014, Moore & Stabeno 2015). A shift has already been observed in the northern Bering Sea benthic communities with northward contractions in dominant species and declines in benthic biomass (Overland & Stabeno 2004, Grebmeier et al. 2006b, Grebmeier et al. 2018). Therefore, monitoring changes in the functioning of the benthos is critical for identifying a larger ecosystem shift.

Various approaches have been used to assess the benthic response to sea ice retreat and food availability on Arctic shelves. Given that sea ice algae accounts for only 4–26% of overall production on Arctic shelves (Legendre et al. 1992, Arrigo 2014), uncertainties remain about the significance of this food source and its potential decline. However, these values may be an underestimate on the Chukchi shelf, where ice algae has been found to significantly exceed phytoplankton biomass and productivity in the spring (Gradinger 2009). Despite the uncertainty in the actual proportion of sea ice algae that supports the benthic based food web, the pulsed

timing and high quality of the largely ungrazed food source is thought to increase its trophic significance (Søreide et al. 2010, Leu et al. 2011, Leu et al. 2015, Dezutter et al. 2019). It has been an ongoing imperative to distinguish the sympagic and pelagic organic matter sources and trace their flow to the benthic and Arctic food webs.

The community composition of ice algae and phytoplankton are complex and have been difficult to unequivocally distinguish since numerous taxa share both environments. Stable isotopes have allowed the detection of an enriched carbon signature in ice algae, yet these values can vary in space and time with bloom progression and may not be reliable indicators alone (Tremblay et al. 2006, Gradinger 2009) and include additional potential sources (e.g. terrestrial, bacterial, etc.). Essential fatty acids are another tool that have advanced our ability to trace organic carbon sources in the Arctic but still lack unambiguous source specificity between the ice and open water regimes (McMahon et al. 2006, Budge et al. 2008, Schollmeier et al. 2018). The use of fatty acids assumes that sea ice organic matter is comprised primarily of diatoms and can best be represented by a fatty acid marker common to diatoms (Budge et al. 2008, Wang et al. 2014). However, the community composition of pelagic blooms is complex and is further compounded by the transition from diatoms to dinoflagellates as blooms progress seasonally in the Pacific Arctic (Szymanski & Gradinger 2016, Hill et al. 2018, Selz et al. 2018). Compound-specific stable isotope analyses of these fatty acids have further refined the distinction between organic carbon sources but still remain equivocal (McMahon et al. 2006, Budge et al. 2008, North et al. 2014, Wang et al. 2014, Kohlbach et al. 2016, Mohan et al. 2016, Kohlbach et al. 2018, Schollmeier et al. 2018).

Highly branched isoprenoids (HBIs) lipids provide an advantage over these other methods to distinguish sympagic and pelagic resources in Arctic food webs. C_{25} HBI lipids are

produced by a small number of commonly occurring diatoms and serve as biomarkers based upon the number and position of double bonds (Volkman et al. 1994, Belt et al. 2007). A monounsaturated C_{25} HBI, termed IP_{25} (Ice Proxy with 25 carbon atoms), is synthesized by three or four sympagic diatom species in the Arctic (Belt et al. 2007, Belt & Müller 2013, Brown et al. 2014b, Limoges et al. 2018). Owing to the stability of this compound and its persistence in the environment, IP_{25} is a reliable proxy for paleo sea ice reconstructions (Stein et al. 2016, Belt 2018). Di- and tri-unsaturated structural isomers provide further context for these interpretations. These isomers include a diene (HBI II), associated with sea ice in both polar regions, and a triene (HBI III), found globally in open waters and marginal ice zones (see review by Belt 2018). HBI III has also proven a reliable pelagic biomarker when used in a sea ice index validated by numerous well-resolved paleo sea ice reconstructions (Müller & Stein 2014, Stein et al. 2017, Kremer et al. 2018). However, modern ecological applications of these HBIs are gaining interest. IP_{25} is chemically stable once grazed and assimilated by consumers, allowing for tracking the trophic transfer of sea ice carbon (Brown & Belt 2012). Measuring the relative proportion of sympagic (IP_{25} and HBI II) to pelagic HBIs (III), creates an index termed H-Print, which provides further insight into resource utilization in Arctic food webs (Brown et al. 2014c).

As with previously described methods, there are limitations to consider with H-Print and the use of HBIs more broadly. In some circumstances, HBI III may be more susceptible to abiotic degradation in the water column based on the extent of algal senescence and the comparative sinking rates of sea ice and open water diatoms, with sea ice diatoms more rapidly removed from the photic zone (Rontani et al. 2019). There is also evidence that HBI III can at times be co-synthesized within or under sea ice (Amiraux et al. 2019). However, this has been attributed to entrapment of pelagic diatoms, as the identified sources of HBI III (from the genus

Rhizosolenia) are not ice-associated and may have been a site-specific phenomenon with minimal impacts on HBI indices. Additionally, the specific assimilation and depuration rates of HBIs in primary consumers are largely unknown. Other studies conclude that HBIs do not bioaccumulate in higher trophic organisms and represent seasonal observations (Brown et al. 2014a, Brown et al. 2017, Brown et al. 2018). However, the advantages of HBIs over previously described methods include the ability to more definitively distinguish sea ice and pelagic carbon sources.

The application of HBI measurements for the Pacific Arctic food web could provide promising new insights into the significance of ice algae on this productive continental shelf system. With this objective in mind, this study applied the H-Print method to track ice algae utilization by benthic consumers of the northern Bering and Chukchi Seas to determine which organisms and/or feeding strategies are more reliant on sympagic carbon. Based on observed shifts in benthic biomass and dominant species along with the phenology and quality of algal blooms the northern Bering Sea over the last decade (Grebmeier et al. 2018), we hypothesize that there are differences in ice algae utilization among feeding strategies and taxa. To test this hypothesis, a range of benthic invertebrates (epifaunal and infaunal) were collected over the summer of 2018 and analyzed for their HBI content with respect to location, feeding strategy and overlying sea ice conditions. Determining the partitioning of sea ice and pelagic organic carbon resources may identify the organisms more vulnerable to a changing food supply as a result of declining sea ice and their ability to adapt to these changes.

Owing to a lack of data on HBI retention and depuration rates in invertebrates, we also conducted a natural depuration experiment using bivalves to determine the turnover rates of HBIs relative to the time of consuming the organic matter. Establishing a baseline of HBI

depuration rates is necessary to accurately estimate the time period of foraging reflected in the H-Print values. Since HBI III is not specific to polar regions, it was practical to measure depuration rates of this HBI from temperate clams. This experimental design allowed us to fully remove natural introduction and prevent recirculation of HBI III using a flow-through filtration system. We used in-situ temperate conditions in Chesapeake Bay, USA because it was not feasible to maintain the flow through system at sustained Arctic temperatures and therefore this experiment serves as a starting point for addressing these questions. We acknowledge that HBI III and IP_{25} may behave differently, but nevertheless this experiment can serve as a general baseline to measure HBI retention in macrofaunal tissue.

2. Materials and methods

2.1. Study site

Sampling locations occurred in regions of high benthic biomass influenced by Pacific water inflow across the shallow (<100 m) continental shelf of the northern Bering and Chukchi Seas (Fig. 1). These regions are annually sampled as part of the Distributed Biological Observatory (DBO), which serves as a change detection array and was formally established in 2010 with time series observations spanning over 30 years (Grebmeier et al. 2010, Moore & Grebmeier 2018). Our sampling spanned five DBO (1-5) regions (https://dbo.cbl.umces.edu) and two additional transects. DBO 1 is located near the winter-only polynya that forms south of St. Lawrence Island in the northern Bering Sea; DBO 2 is in the Chirikov Basin south of Bering Strait; DBO 3 is in the southeast Chukchi Sea, where organic rich material settles out north of Bering Strait; DBO 4 is in the northeast Chukchi Sea on the southeastern flanks of Hanna Shoal; and DBO 5 is a transect across Barrow Canyon (Grebmeier et al. 2015). Icy Cape (IC) has high benthic biomass

due to sustained advection of organic carbon from more productive regions (Feder et al. 1994). The Ledyard Bay (LB) transect is in the Chukchi Sea and was only sampled for surface sediments.

2.2. Sea ice persistence

Sea ice persistence data were determined from sea ice concentrations obtained from the Special Sensor Microwave Imager/Sounder (SSMIS) on the Defense Meteorological Satellite Program satellites, and compiled by the National Snow and Ice Data Center (http://www.nsidc.org). A 15% ice concentration threshold was set to identify days of sea ice presence in the Pacific Arctic region (Frey et al. 2015). We then summed the number of days with sea ice present (>15%) per pixel, from 14 September 2017 through 15 September 2018. Discrete sea ice persistence values were obtained for each of the sampling locations by extracting the value of the pixel at each location (Fig. 1). The use of annual persistence, rather than confined to the sampling period, allowed for the inclusion of winter sea ice conditions that would contribute to the lack of or delay in a spring bloom and account for the deposition of organic matter available in the sediments prior to sampling.

2.3. Benthic sampling

Organisms were collected on board the CCGS *Sir Wilfrid Laurier* (SWL18; 16–23 July 2018) and the USCGC *Healy* (HLY18-01; 7–24 August 2018) as part of the DBO program (Table 1, Fig. 1). Additional samples were collected opportunistically on board the R/V *Sikuliaq* (SKQ2018; 4–25 June 2018) as part of the Arctic Shelf Growth, Advection, Respiration and Deposition (ASGARD) Rate Measurements Project of the Arctic Integrated Ecosystem Research Program, which overlapped with the DBO 2 and 3 regions (Table 1, Fig. 1).

Epibenthic megafauna were collected from trawl surveys on SKQ2018 using a modified plumb-staff beam trawl (2.26-m opening; 7-mm mesh net; 4-mm cod end liner). Trawl sample biomass was dominated by echinoderms, mollusks, crustaceans, sponges, ascidians and bryozoans. Organisms were either sorted from the full catch or from a well-defined, well-mixed subsample. All samples were sorted by species, genus or distinct morphotype depending on the level of identification possible on board. Surface sediments were not collected on this cruise.

Benthic macrofauna (> 1 mm, included megafauna) were collected on the SWL18 and HLY18-01 cruises using a 0.1 m^2 van Veen grab weighted with 32 kg lead. Grab sample biomass was dominated by bivalves, polychaetes, crustaceans, sipunculids, echinoderms and anthozoans. The grab was gently lowered on to the deck and a trap door on the top was opened prior to the full grab opening in order to sample relatively undisturbed surface sediments for HBI analysis. The sediments were collected by skimming the surface with a metal spatula. Prior studies have established from radiocesium activities that the surface sediments on the Bering and Chukchi shelf (<100 m) reflect recent deposition, and that due to bioturbation, surface sediments recovered from the tops of cores are as well-mixed as those from the tops of van Veen grabs (Cooper et al. 1998, Cooper & Grebmeier 2018). Organisms were sieved through 1-mm mesh sieve screens, live sorted and identified to the lowest taxonomic level practical on board. Organisms from all three cruises and sediments were placed in individual whirl-pak bags, immediately frozen (-20°C) and stored until analysis. All benthic fauna collected were classified by feeding strategy using the following five categories: suspension (SUS), surface deposit feeder (SDF), sub-surface deposit feeder (SSDF), suspension-surface deposit (SUS/SDF), or predator/scavenger (PS) based on previous studies (Table 2).

2.4. Biomarker extraction

All samples were freeze dried in the laboratory for 48 hours, soft tissues were removed from shells as required, and homogenized by mortar and pestle. Approximately 1 g of dried sediment or 0.1–0.5 g of dried tissue were subsampled for analysis. Owing to the variable sizes and number of organisms per station, where there was often only one individual per taxon per grab, major taxa with more than one individual were grouped for analysis. This was intended to capture a representative HBI composition per species and/or feeding strategy at a particular station. HBI biomarkers were extracted from 78 surface sediment samples and 193 tissue samples. HBIs were extracted following established methods (Belt et al. 2012, Brown et al. 2014c). Briefly, an internal standard (10 µL) of 9-octylheptadec-8-ene (9-OHD, 1 µg mL^{-1}) was added to the sample before extraction to facilitate yield quantification. Samples were saponified in a methanolic KOH solution and heated at 70°C for one hour. Hexane (4 mL) was added to the saponified solution, vortexed, and centrifuged for three minutes at 2500 RPM, three times. The supernatant with the non-saponifiable lipids (NSLs) was transferred to clean glass vials and dried under a gentle N_2 stream. We removed elemental sulfur from the sediment samples following established protocols (Koch et al. 2020) to prevent analytical interference with HBI III. The initial extracts were re-suspended in hexane and fractionated using open column silica gel chromatography. The non-polar lipids containing the HBIs were eluted while the polar compounds were retained on the column. The eluted compounds were dried under N_2. 50 µL of hexane was added twice to the dried purified extract and transferred to amber chromatography vials.

2.5. Biomarker analysis

The extracts were analyzed using an Agilent 7890A gas chromatograph (GC) coupled with a 5975 series mass selective detector (MSD) using an Agilent HP-5ms column (30 m x 0.25

mm x 0.25 µm), following established methods (Belt et al. 2012). The oven temperature was programmed to ramp up from 40°C to 300°C at 10°C/minute with a 10-minute isothermal period at 300°C. HBIs were identified using selective ion monitoring (SIM) techniques. The SIM chromatograms were used to quantify the HBI abundances by peak integration with ChemStation software. A purified standard of known IP_{25} concentration was used to confirm the mass spectra, retention time and retention index (RI). The HBIs were identified by their mass ions and RI including IP_{25} (*m/z* 350.3), HBI II (*m/z* 348.3) and HBI III (*m/z* 346.3). A procedural blank was run every 9th sample. Individual HBI concentrations in the surface sediment samples were normalized by total organic carbon (TOC) on an organic gram weight basis. Surface sediment TOC data from the SWL18 and HLY18-01 cruises were accessed from the National Science Foundation's Arctic Data Center (Grebmeier & Cooper 2019b, c).

The H-Print index was used to provides an estimate of the relative organic carbon contributions of phytoplankton to sea ice algae (Brown et al. 2014c). The H-Print (eq. 1), is calculated using the relative abundances of IP_{25}, HBI II and HBI III, as determined by GC-MS methods:

$$\text{H-Print \%} = \frac{\text{HBI III}}{\sum (\text{IP}_{25} + \text{HBI II} + \text{HBI III})} \text{ x } 100 \qquad (1)$$

The estimated organic carbon contribution varies from 0% to 100%, with lower values indicative of proportionally greater sympagic organic carbon and higher values indicative of proportionally greater pelagic organic carbon. Analytical error from replicate control tests was determined to be less than 3% for H-Print values in an individual organism from homogenized tissue sample. Sea ice organic carbon (iPOC), as a proportion of marine-origin carbon within samples, was

estimated using Eq. 1 from a prior H-Print calibration from feeding experiments with known algal species ($r^2 = 0.97$, $p < 0.01$; Brown & Belt 2017).

$$\text{iPOC \%} = 101.08 - 1.02 \times \text{H} - \text{Print} \qquad (2)$$

Given our interest in the proportion of sea ice algae utilization, the iPOC calibration is presented referenced to sea ice carbon rather than pelagic carbon, as is the case with the H-Print. However, since the calibration was derived and validated from feeding experiments, we retained the H-Print values for the sediment data. Therefore, all invertebrate samples were converted and reported as iPOC, while sediments are reported as H-Print.

2.6. Statistical analysis

All statistical analyses were performed in R v. 3.6.1 (R Core Team 2017). Normality of the data was assessed using a Shapiro-Wilks test and the homogeneity of variance using Levene's test. We used a generalized additive model (GAM) in R using package 'mcgv' to determine the effects of various predictor variables for the sea ice organic carbon content in benthic macrofauna. This included sea ice persistence, sampling location, feeding strategy and sediment H-Print composition. A combination of these variables in seven competing equations was evaluated and the best performing equation was selected based on the lowest AIC (Akaike information criterion) score. Linear regression models were assessed to determine the relationship between the HBI content of invertebrate tissue (iPOC%) and the corresponding surface sediment (H-Print %) they were collected from. We conducted k-means clustering analysis to group similar observations and assess potential patterns in the HBI distribution among location, feeding strategy, major taxa and annual sea ice persistence. Owing to the lack of corresponding sediment samples, the samples collected from SKQ2018 (n = 41) were not included in the cluster analysis. We then used the combination of factors that explained the

variation within the benthic macrofauna samples by the GAM to define the individual clusters. This analysis was conducted in R using packages 'cluster' and 'factoextra'. Sediment H-Print and macrofauna iPOC values were normalized prior to running the cluster analysis and the optimal number of clusters (k) were determined based on the gap statistic (Tibshirani et al. 2001). One-way ANOVA with Tukey Honest Significant Difference (HSD) and Bonferroni corrections were used to analyze the significant differences in relative HBI concentrations.

2.7. HBI depuration experiment

In May 2019, bivalves were collected from the pier at the Chesapeake Biological Laboratory (CBL) in Solomons, Maryland, USA using a hand-deployed PONAR grab. The two species collected are widely distributed and also found in parts of the Arctic, *Mya arenaria* (suspension feeder, n= 18) and *Macoma balthica* (suspension and surface deposit feeder n = 50). *M. balthica* (n=10) and *M. arenaria* (n=3) were analyzed immediately (day 0) after collection to determine their initial HBI III content from their natural environment and the remainder (*M. arenaria*, n = 15; *M. balthica*, n = 40) were put in flow through filtered seawater tanks (5L). The clams were fed every other day with Shellfish Diet 1800 (Instant Algae, Reed Mariculture). The Instant Algae (1 mL) was analyzed prior to feeding to confirm there were no HBIs present.

Clams were removed from the tank and the HBI III abundances were analyzed at 4, 7, 21, and 28 days. Owing to the small size of the individual *M. balthica* collected (~5 mm), individuals had to be grouped (n=10 per collection date) for analysis. The *M. arenaria* samples were a sufficient size (~20–30 mm) for individual analysis (n=3 per collection date). The relative response on the GC-MS was recorded until the response fell below detection limits, indicating complete depuration of the biomarkers. As the depuration rate was the intended measurement, absolute quantification of HBI III was not undertaken.

3. Results

Several factors were considered in various combinations to explain the variation observed in sea ice organic carbon utilization among benthic macrofauna. The GAM equation selected was based on the AIC scores, with the lowest AIC indicating the best fit. The combination of sample region, sea ice persistence, sediment H-print, and feeding strategy performed the best (AIC=1140, r^2=0.78). Therefore, the following variables were examined in greater detail.

3.1. Surface sediment HBI distributions and relationship with sea ice

IP_{25} was only detected in trace amounts as a fraction of organic carbon (OC; < 1 µg g OC^{-1}) throughout DBO 1–2 in the northern Bering Sea and less than 2 µg g OC^{-1} was observed at DBO 3 in the southern Chukchi Sea (Fig. 2A). Ledyard Bay (LB), which was only sampled for sediments, marked a transitional zone where IP_{25} levels increase in the northeast Chukchi Sea. IP_{25} reached maximum concentrations of 14.5 µg g OC^{-1} in the northeast Chukchi Sea at DBO 4 and ranged from 1 to 10 µg g OC^{-1} at the DBO 5 transect across Barrow Canyon. HBI III (Fig. 2B) displayed a more homogenous distribution throughout the region. Localized areas of elevated concentrations were observed in LB, where HBI III reached 18 µg g OC^{-1}. HBI III levels were also considerably lower in the northern Bering Sea at DBO1–2 with values ranging from 2–6 µg g OC^{-1}. H-Print (Fig. 2C) follows a latitudinal gradient from south to north with decreasing relative pelagic HBI inputs. The mean sea ice extent indicates that the IC transect was ice-covered in June but retreated by July, while the sea ice had fully retreated from DBO 4 and 5 by August.

There was a significant relationship between sea ice persistence and sediment H-Print (r^2=0.61, $p < 0.001$; Fig. 3). The DBO 1 stations experienced low (<30 days) sea ice cover in

2018 and were determined to be outliers using a Grubbs' test (Grubbs 1950) (Fig. 3 red-dashed box). After removing the subset of DBO 1 samples (n=3), the strength of the relationship increased, indicating a very strong fit (r^2=0.81, $p < 0.001$).

3.2. Sea ice organic carbon (iPOC %) variation by feeding strategy and region

There was an increasing gradient of sympagic utilization by benthic invertebrates from the lower latitude sampling regions (DBO 1–3) to the higher latitude sampling regions (IC and DBO 4–5; Fig. 4). The invertebrates classified as deposit feeders (both SDF and SSDF) generally had the highest iPOC and SUS the lowest within each region. The highest iPOC values are observed in the SSDF category. However, the SDF at DBO 5 (most northerly sampling area) reach iPOC levels similar to SSDF. The highest iPOC value observed among the SDF at DBO 5 (78%) was comparable with the SSDF and attributed to sipunculids (*Golfingia margaritacea*). iPOC values increased at the IC transect. iPOC values for SUS fauna were <25% in all sampling regions, with the exception of DBO 4, indicating that they are utilizing predominantly pelagic resources. P/S by comparison have a less clear trophic dependence on sympagic sources relative to the other feeding strategies from DBO 1–3. The SUS/SDF align with SUS but with greater differences at IC and DBO 5. Feeding strategies were significantly different ($p < 0.05$) at all stations but DBO 1 and 2 as determined by one-way ANOVA testing (Table 3). Tukey HSD pairwise comparisons indicate SUS were significantly different from deposit feeders (SDF and SSDF) at all four of these sampling regions (see Table S1 for *p*-values).

3.3. Relationships between macrofauna iPOC and sediment H-Print

The linear regression of normalized iPOC values for the invertebrate tissues and corresponding H-Print values in surface sediments indicates a significant relationship between

these variables ($p < 0.001$, $r^2=0.66$). The samples were grouped into 3 clusters (Fig. 5A). The cluster composition took advantage of the prior assessments of the factors determined to be significant (e.g. DBO region and feeding strategy, Figs. 5B and 5C, respectively). Sea ice persistence patterns and taxa composition were also examined for each of the clusters.

Cluster 1 samples were found throughout the Chukchi Sea including DBO 3, DBO 4, DBO 5 and IC (Fig. 5B) with a majority (52%) from IC (Table 4). The difference in feeding strategy was not significant based on a one-way ANOVA test (Table 3). The composition of feeding strategies contained in cluster 1 (Fig. 5C) was distributed among SUS (38%), SSDF (28%), SUS/SDF (17%), SDF (3%), and PS (14%; Table 4). The SSDF group had the highest mean iPOC (23 ± 9%) and SUS had the lowest (10 ± 9%; Fig. S1). This cluster was dominated by bivalves (62%) and polychaete worms (21%). Overall, cluster 1 had a moderate sediment H-Print (42 ± 11%) with invertebrate iPOC values indicative of low sea ice organic carbon utilization (mean iPOC 17 ± 10%; Table 4). The mean sea ice persistence for this cluster was 205 ± 35 days (Table 4).

Cluster 2 stations were located in the northeast Chukchi Sea from IC, DBO 4 and DBO 5 (Fig. 5B), with the majority from DBO 4 (66%; Table 4). The organisms sampled in this cluster were predominantly SSDF (57%; Table 4). Two of the three SUS samples included in this cluster (bivalve *Astarte borealis* and amphipod *Ampeliscia* sp.) were from a station in DBO 4 with high IP_{25} deposition (DBO 4.4). Feeding strategy was found to be significant based on the one-way ANOVA test ($p < 0.05$; Table 3). The iPOC values in this cluster were highest overall. Values ranged from 37-57%, with SSDF the highest (57 ± 11%) and SUS/SDF the lowest (37 ± 3%; Fig. S1). The Tukey HSD pairwise comparison indicated that SUS/SDF–SSDF and SUS–SSDF were significantly different ($p < 0.05$; Table S1). Cluster 2 contained bivalves (52%) and polychaete

worms (25%), but also an increased contribution from sipunculids (9%; Table 4). The mean sediment H-Print was low (i.e. sympagic) at 29 ± 7%, with invertebrate iPOC values ranging from moderate to high with a mean value of 53 ± 12% (Table 4). The mean sea ice persistence was the longest of all clusters at 227 ± 18 days of the year (Table 4).

Cluster 3 contained the northern Bering Sea (DBO 1 and 2) and southeast Chukchi Sea (DBO 3) stations, immediately north and south of Bering Strait (Fig. 5B). 63% of the samples in cluster 3 were from DBO 3, but contained all samples from DBO 1 and 2 (Table 4). Feeding strategy was a significant variable for this cluster based on one-way ANOVA tests ($p < 0.001$; Table 3). SUS (27%), SSDF (35%) and SUS/SDF (27%) were the primary feeding strategies within this cluster (Table 4). SDF had the highest mean iPOC value (13 ± 6 %) with SUS the lowest at 1 ± 3%, meaning food sources were nearly completely pelagic (Fig. S1). The differences were significant between SUS–PS ($p < 0.05$), SUS–SDF ($p < 0.01$) and SUS–SSDF ($p < 0.001$) based on pairwise comparisons (Table S1). Cluster 3 was dominated by bivalves (52%) and polychaetes (27%), with an increased contribution from ampeliscid amphipods (13%; Table 4). The mean sediment H-Print was high (80 ± 5%, i.e. pelagic) and the mean iPOC value in invertebrate tissues was low (5 ± 5%; Table 4). The sea ice persistence for cluster 3 was the shortest at 111 ± 55 days (Table 4).

3.4. Sea ice persistence and sea ice organic carbon (iPOC %)

The clusters were further analyzed using the linear regression of sea ice persistence determined from each of the sampling locations relative to the invertebrate tissue iPOC (Fig. 6A). The clusters remain distinctly grouped with the exception of two data points from cluster 1. The relationship between sea ice persistence and sea ice carbon utilization was significant ($p < 0.001$, $r^2 = 0.41$; Fig. 6A). However, there was a distinct group from cluster 3 with stations that

experienced less than 30 days of sea ice, including several samples where there was no sea ice cover in 2018 (Fig. 6A, red-dashed box). By removing this cluster from the linear regression, the fit of the relationship improved ($r^2 = 0.56$, $p < 0.001$). All of the stations with no or low sea ice cover occurred at DBO 1, also known as the St. Lawrence Island polynya (SLIP) region (Fig. 6B). Stations SLIP 1 and SLIP 2 had no sea ice cover during the study period in 2017-18, while SLIP 3 and SLIP 5 had less than 30 days of sea ice. The SDF and SUS/SDF iPOC were lowest at SLIP 1 and 2, with values at or near 0%. The SSDF and P/S iPOC values are slightly higher, but still consistent with dominantly pelagic organic carbon acquisition (<20% sea ice organic carbon). The patterns are less clear at SLIP 3 and 5, with both SSDF and SUS sea ice organic carbon sources less than 10% and a group of SSDF, SDF and SUS/SDF falling between 6–18% (Fig 6B).

3.5. Sea ice organic carbon (iPOC %) utilization by major taxa

The species that contained the highest iPOC values (>75%) included maldanid polychaetes, the sipunculid *G. margaritacae*, and the clam *Ennucula tenuis* (Fig. 7A). High levels of iPOC (50–75%) were observed in the clams *Yoldia hyperborea* and *Macoma calcarea*, brittle star *Ophiura sarsii*, polychaete *Pectinaria hyperborea*, amphipod family Lysianassidae (not practical to identify species at sea), and sea star *Henricia* sp. Moderate iPOC levels (25–50 %) were observed in the clams *Nuculana pernicula* and *Astarte borealis*, gastropod *Buccinum scalariforme*, and amphipod *Ampeliscia* sp. The lowest iPOC levels (<25%) occurred in the snow crab *Chionoecetes opilio*, predatory polychaete *Nepthys* sp., bivalves *Serripes laperousii* and *Mya* sp., and all tunicates, holothuroids, ascidians, anthozoans, and the remaining gastropods. Estimates of iPOC by feeding strategy (Fig. 7B) reveal a dominance of SSDF in the dominant utilization of sea ice organic carbon (iPOC >50%). The SDF organisms were primarily

in the moderate to high range of iPOC, but also contained the highest mean iPOC values (e.g. sipunculids and brittle stars). None of the suspension feeders exceeded use of more than 25% sea ice carbon.

3.6. HBI depuration rates

The depuration rates determined from the temperate clam experiment suggest similar timing for suspension/deposit feeding *M. balthica* and suspension feeding *M. arenaria* at 21 and 28 days respectively (Fig. 8). Relative HBI III abundance indicated reductions by day 7 in both species, however there were detectable levels until the 3 to 4-week sampling events.

4. Discussion

The spatial distribution of H-Print in surface sediments in 2018 (Fig. 2C) followed a latitudinal gradient previously observed for the region (Koch et al. 2020). IP_{25} concentrations were relatively high in surface sediments in the northeast Chukchi Sea compared to previous years, exceeding 14 µg g OC^{-1} (Fig. 2A). The strong relationship between sea ice persistence and sediment H-Print supports the use of these biomarkers in this region as diagnostic of sea ice cover (Fig. 3). Based on the distribution of HBIs, we hypothesized that the invertebrate HBI composition would be influenced by the regional HBI patterns in the surface sediments as indicators of available food sources. Linear regressions between sediment H-Print and macrofaunal iPOC confirmed that location was a significant influence (Figs. 4, 5C).

Sea ice persistence, which was correlated with DBO region, appeared to be an important factor in the cluster analysis. The samples in cluster 3 were located in the three southern DBO regions (Table 4; Fig. 5). Baseline studies of H-Print in Pacific Arctic surface sediments suggest that a dominance of pelagic carbon is common throughout these three DBO regions (Koch et al.

2020). However, a defining feature of this region in 2017-2018 was the record low maximum sea ice extent (Grebmeier et al. 2018, Stabeno & Bell 2019). This may be the reason for the outlier iPOC signatures from benthic macrofauna samples collected at SLIP 1 and SLIP 2, where there was no sea ice cover and presumably no freshly deposited ice algae (Fig. 6A-B). The large ice-edge bloom that typically occurs in April or May over the northern Bering shelf did not occur in 2018, according to primary production measurements derived from satellite observations of chlorophyll *a* (Frey et al. 2018). The late pelagic bloom and abnormally low chlorophyll in the northern Bering Sea near DBO 1 were observed from fluorescence sensors on the M5 mooring (Duffy-Anderson et al. 2019). The lack of sea ice also led to bottom water temperatures that were above 0°C for the first time since observations began in 1988 (Grebmeier & Cooper 1995, Grebmeier et al. 2018), eliminating the cold pool that typically serves as a thermal barrier to several pelagic and demersal fish species that could alter benthic food webs (Grebmeier et al. 2018, Duffy-Anderson et al. 2019). An observed ecosystem shift in this region has occurred over the last few decades, including a northward shift in benthic biomass and decline of nuculanid and nuculid bivalves replaced by maldanid polychaetes (Grebmeier et al. 2006b, Grebmeier et al. 2018). There has also been a northward contraction of the bivalve *M. calcarea* within the sampled stations in DBO 1 (Goethel et al. 2019). A recent study concluded that physical oceanographic shifts in this system are largely responsible for driving the changes seen in benthic community structure (Waga et al. 2020), and it seems plausible that these shifts are likely connected to changing food sources in the northern Bering Sea.

Moving northward, cluster 1 had a majority of the IC samples and a subset of samples from DBO 5 (Table 4; Fig. 5). The IC transect was located at the approximate position of the ice-edge through June and July before the rapid retreat off of the Chukchi shelf by August (Fig. 2C).

At this location, the ice retreats in an onshore to offshore pattern with sea ice persistence lower by 20–30 days at the onshore sampling locations. This transect is also located at the start of the Central Channel for Bering Sea water transport northwards and current flow increases, as indicated by coarser grain sizes (Grebmeier & Cooper 2019c), suggesting reduced deposition of particulate organic matter including ice algae and phytoplankton. The sea ice persistence patterns, location of the mean ice edge for June and July, and sediment H-Print values show a clear delineation between IC and DBO 4 despite their relatively close proximity (Figs. 1–2). There is also a front that forms between these regions, keeping warmer, nutrient poor Alaska coastal water south and offshore and nutrient-rich Bering Sea water to the north near DBO 4 (Weingartner et al. 2017). The strong negative correlation between sea ice persistence and H-Prints suggest that the additional approximate month of sea ice at DBO 4 driven by the hydrography had an impact on IP_{25} synthesis and deposition. The surface deposit feeders at IC also contributed to the elevated iPOC values associated with this cluster (Fig. 4). The DBO 5 line is a transect across Barrow Canyon. The H-Prints are elevated in the center of the canyon (~35%), yet still dominantly sympagic, and decrease on the sides (~14-18%). We attribute this cross-sectional pattern to the flow through Barrow Canyon, where currents converge with mean speeds of 15-20 cm/s (Bering water) and surface currents upwards of 70–100 cm/s (Alaska Coastal Current on the eastern flanks) with bottom intensified flows (Aagaard & Roach 1990, Pickart et al. 2005, Pickart et al. 2019). Although Barrow Canyon is on the northeast Chukchi Shelf where ice algae influence is most significant, ice algal aggregates likely do not settle to the bottom of Barrow Canyon as readily because of stronger currents than on the shelf and organic materials are transported towards the basin because of these enhanced current speeds (Lepore et al. 2009). Additionally, the high current speeds in Barrow Canyon favor suspension over deposit

feeding (Pisareva et al. 2015). Therefore, the reason for these DBO 5 samples to be clustered with IC is likely due to the apparent increased phytoplankton utilization by suspension feeders relative to DBO 4 (Fig. 4).

As previously noted, DBO 4 and 5 dominated the cluster 2 composition in the northeast Chukchi Sea where ice algae deposition and utilization were most substantial. There were fewer SUS and P/S collected within the offshore DBO 4 transect. Macrofaunal biomass at these sites is typically dominated by deposit feeders, primarily sipunculids and maldanid polychaetes, but also brittle stars (Ophiuridae) and bivalves (Yoldiidae and Astartidae) and occasionally the SUS/SDF bivalve *M. calcarea* (Grebmeier & Cooper 2019a). Depositional regimes on the Chukchi shelf, such as along DBO 4, tend to favor deposit feeders over suspension feeders (Pisareva et al. 2015). The HBI data show that the pairing of longer sea ice persistence in a depositional environment results in higher ice algae utilization. Recent studies indicated that IP_{25} and diatom export occur year-round at this location (Koch et al. 2020, Lalande et al. 2020). There is currently a lack of HBI flux data available from other DBO regions, but preliminary HBI data from sediment traps at DBO 2 and DBO 3 suggest this steady supply of sympagic HBIs is likely a unique feature at DBO 4 (unpublished data, C.W. Koch). Although pelagic phytoplankton blooms are greater in the summer as seasonal ice retreats, in addition to the occurrence of under-ice phytoplankton blooms (Arrigo et al. 2014, Assmy et al. 2017), the continuous export of IP_{25} suggests a sustained source of sea ice carbon is transported to the benthos, both when grazing pressure in the water column is minimal and as a result of re-suspension events throughout the year (Koch et al. 2020). The mean iPOC value in the invertebrate tissue samples suggests an approximate 50:50 mixture of ice algae and phytoplankton, although our analysis does not preclude organic carbon from other possible detrital or terrestrial sources. Feeding experiments

providing both ice algae and phytoplankton to benthic consumers have shown that certain organisms may preferentially consume ice algae (McMahon et al. 2006, Sun et al. 2009). It has also been suggested that despite the preference for ice algae, many Arctic macrofauna exhibit dietary plasticity and will respond similarly to availability of either category of organic matter and may not be dependent on ice algae (Mäkelä et al. 2017, Kędra et al. 2019).

Location did not fully account for the variability among the sampled organisms and was the basis for exploring the differences among species and feeding strategies. Deposit feeders have been previously observed to have greater ice algae utilization than suspension feeders based upon fatty acid concentrations in macrofaunal tissues in the Chukchi Sea (Schollmeier et al. 2018). This was similarly demonstrated through feeding experiments and was attributed to preferential grazing on the higher fatty acid composition of ice algae (McMahon et al. 2006). Our iPOC measurements confirm these findings, with higher values for surface and subsurface deposit feeders than suspension feeders throughout the study area (Fig. 4). Our HBI measurements do not mean that suspension feeders do not utilize ice algae from the water column. However, because ice algae aggregates sink rapidly to the seafloor and can overwhelm any pelagic grazers present, it is possible that much of the ice algae is not immediately consumed but is incorporated into the surface sediments (Legendre et al. 1992). By contrast, suspension feeders may more predominantly depend on water column phytoplankton that can be suspended in the water column over longer periods of the seasonal cycle.

Understanding HBI retention in consumers is critical to fully interpreting any transition in food sources as sea ice coverage diminishes. Short residence times (days to weeks) of HBIs in various consumer tissues have been suggested from previous studies (Brown & Belt 2012, Brown et al. 2013b, Brown et al. 2014a). Based on the results from the HBI III depuration

experiment (Fig. 8), and the assumption that those temperate results are generalizable to higher latitudes, the HBI signal may represent assimilation over the course of approximately one month prior to sampling. Similar assimilation rates (i.e. approximately one month) of organic carbon were determined in Arctic bivalves using isotope labeled ice algae (McMahon et al. 2006). While IP_{25}-specific depuration rates are currently unavailable, a starting point might be to assume that this compound would behave similarly to HBI III, with further experimentation required to confirm this. Complexities include prior studies that suggest that metabolic rates can be quite variable in response to seasonal variations in temperature (Jansen et al. 2007) or that Arctic bivalves use elevated metabolic rates at low temperatures as an adaptation strategy (Thyrring et al. 2015). The potential influence of temperature on metabolic rates when comparing our experiment using temperate species with Arctic species clearly imposes some limitations on the extent of possible interpretation. However, the results of this experiment demonstrate that very short lipid depuration (i.e. less than 48 hours) or bioaccumulation were not observed. If either were to be the case, relationships between sea ice and organic carbon transfer to higher trophic levels would be more ambiguous to interpret.

Ice algae deposition occurred with the shortest time interval in the northeast Chukchi Sea stations prior to sampling, allowing for the freshest deposition of iPOC at those locations. Owing to the low sea ice conditions in the Bering Strait region in 2018, there would have been little to no opportunity for ice-associated blooms, as was evident in the anomalous timing of maximum chlorophyll biomass in June rather than April–May (Frey et al. 2018). Therefore, the low levels of iPOC in deposit feeders from DBO1 and 2 (Fig. 6B) were most likely from previous years' sea ice carbon stored in the sediments. This indicates that this carbon source may serve as a reserve of lipid-rich organic matter in low sea ice years. This "sediment food bank" on polar

shelves has been supported by other studies (Mincks et al. 2005, Pirtle-Levy et al. 2009, Sun et al. 2009, McTigue & Dunton 2014, North et al. 2014, Schollmeier et al. 2018). Analysis of HBIs from sediment cores on the Chukchi Shelf indicate that IP_{25} is well-mixed by bioturbation and can increase with depth (Koch et al. 2020). However, biological utilization of stored sea ice carbon and consistent burial through bioturbation will ultimately deplete these reserves, and subsequently the associated sympagic HBIs.

The importance of ice algae to predators and scavengers is not clear in light of our results. The iPOC values of these organisms suggest ice algae may not be a significant component of their diet, which indicates more about their available prey items. It appears that P/S had comparable sea ice organic carbon levels as deposit feeders at IC (Fig. 4). Unfortunately, our sample sizes at DBO 4 and 5 were too low to robustly investigate this relationship where ice algae is incorporated into tissues in greater proportions. Future studies focused in these locations to analyze the progression of iPOC values in P/S and their preferred prey following sea ice retreat would be useful to better understand the significance of ice algae sources to these organisms, as they serve as important trophic links in the Pacific Arctic food web (Bluhm et al. 2009).

The SUS/SDF tellinid clams (e.g. *M. calcarea*), have a wide range of iPOC values. *M. calcarea* are found throughout the Pacific Arctic region and often dominate the macrofaunal biomass (Grebmeier et al. 2018). Their dietary plasticity is advantageous to allow for broader utilization of the available food source. The range of iPOC values of *M. calcarea* were between those of the deposit and suspension feeders, suggesting utilization of dual feeding strategies. Prior work found that *Macoma* species preferred ice algae over phytoplankton (Sun et al. 2009), but compound specific stable isotope analysis of amino acids has also revealed that some deposit

feeding benthic species with high feeding plasticity can adjust feeding strategies in response to the quality and availability of organic matter reaching the seafloor (Kędra et al. 2019). One other species in this study, *G. margaritacea* (Sipuncula), is primarily a deposit feeder in the Pacific Arctic but also capable of suspension feeding (Gibbs 1977, Kędra et al. 2018). Sipunculids may utilize this feeding method in high current flow regions like that of Barrow Canyon where sipunculan abundance is high (Kędra et al. 2018).

G. margaritacea was one of two species in which the low end of the interquartile range of iPOC values was in the moderate utilization category for ice algae (25–50%, Fig. 7B). It also had one of the highest mean iPOC values overall. This range of iPOC values suggests that *G. margaritacea* is one of the benthic macrofaunal groups most reliant on ice algae in the Pacific Arctic. *G. margaritacea* abundance is greater in the Chukchi Sea than in the northern Bering Sea, particularly in depositional environments, which may be driven by sea ice persistence and differing food types reaching the seafloor (Kędra et al. 2018). Our results also suggest there may be an association between ice algae deposition and sipunculan distributions. Sipunculids are a known prey item for important higher trophic organisms including the Pacific walrus (Sheffield & Grebmeier 2009, Jay et al. 2014), snow crab (Divine et al. 2017), and possibly others (Kędra et al. 2018). We also found that the brittle star *O. sarsii* had elevated sea ice algae dependence relative to other species. Elevated ice algae utilization by ophiuroids has been observed in the Canadian Arctic using HBIs, stable isotopes and fatty acids (Kohlbach et al. 2019). *O. sarsii* are widely distributed throughout the Pacific Arctic, however, they are most abundant in the northern Chukchi Sea than to the south (Ambrose et al. 2001, Bluhm et al. 2009) although they are also abundant in the muddy sediments on the outer shelf-slope southwest of St. Lawrence Island (Grebmeier et al. 2015). Brittle star abundance is associated with finer grain sizes

(Grebmeier et al. 2015), but our HBI data suggest that it could also be influenced by the availability of ice algae as a food source in these depositional environments. *O. sarsii* are also a prey item for snow crab in addition to sea stars and buccinid snails (Bluhm et al. 2009), which are similarly important trophic links to marine mammals. Despite the suggestion of potential plasticity to food quality and availability, based upon biomarker evidence, sipunculids and brittle stars seem to have a preference for ice algae and may face greater impacts to shifting food sources as seasonal sea ice coverage is reduced.

5. Conclusions

The main goal of this study was to determine the relative importance of ice algae on the highly productive shelves of the Pacific Arctic. The detection of sea ice source-specific biomarkers IP_{25} and HBI II, in comparison to the pelagic-sourced HBI III biomarker, suggests that both surface and subsurface deposit feeders in this region are more reliant on ice algae, compared to suspension feeders and predators/scavengers. Sea ice carbon is more abundant and utilized in greater proportions in the northeast Chukchi Sea relative to the northern Bering Sea and Bering Strait regions to the south. Our findings indicate that benthic communities of the Pacific Arctic display dietary plasticity for both sea ice and pelagic food sources with elevated ice algae utilization across several taxa and feeding strategies, either driven by elevated lipid content or availability and accessibility of this food source. Changes in quality, quantity and timing of primary production are likely to impact these benthic populations. The concept of a food bank stored within sediments on Arctic shelves is further supported here. This reservoir of organic matter may provide prolonged access to lipid reserves in the sediment in low sea ice years and in the decades to come. If ice algae production becomes much less prominent as the ice edge retreats northward, the sympagic carbon reserves will eventually be depleted and

replaced by exclusively pelagic-sourced carbon which may particularly affect those organisms that currently obtain nearly half of their carbon from ice algae. The incorporation of HBI measurements into Arctic benthic food web studies provides advantages as a monitoring tool because of the source-specificity associated with the sea ice origin of organic matter. While the HBI measurements improve our ability to track the utilization of sea ice primary production, they may not fully capture the pelagic primary production and might be best considered complementary measurements to other diagnostic analyses such as stable isotopes and essential fatty acids.

6. Acknowledgements

We thank the captains and crew aboard the CCGS *Sir Wilfrid Laurier* and USCGC *Healy*. We also thank Katrin Iken (University of Alaska Fairbanks) for epibenthic sample collection and identification from the ASGARD cruise on the R/V *Sikuliaq*. We thank the four anonymous reviewers for their constructive comments that helped improve an earlier version of the manuscript. Financial support was provided by grants from the U.S. National Science Foundation Arctic Observing Network program (Award # 1917469 to J. Grebmeier and L. Cooper and Award # 1917434 to K. Frey) and NOAA Arctic Research Program (CINAR 22309.07) to J. Grebmeier and L. Cooper. We thank the North Pacific Research Board (NPRB) for additional funding support provided to C. Wegner (Koch) through the NPRB Graduate Research Award.

7. References

Aagaard K, Roach A (1990) Arctic ocean-shelf exchange: Measurements in Barrow Canyon. Journal of Geophysical Research: Oceans 95:18163-18175. https://doi.org/10.1029/JC095iC10p18163

Ambrose W, Clough L, Tilney P, Beer L (2001) Role of echinoderms in benthic remineralization in the Chukchi Sea. Marine Biology 139:937-949. doi:https://doi.org/10.1007/s002270100652

Arrigo KR (2014) Sea ice ecosystems. Ann Rev Mar Sci 6:439-467. doi:10.1146/annurev-marine-010213-135103

Arrigo KR, and Gert L. van Dijken (2015) Continued increases in Arctic Ocean primary production. Progress in Oceanography 136:60-70. doi:10.1016/j.pocean.2015.05.002

Arrigo KR, Perovich DK, Pickart RS, Brown ZW, van Dijken GL, Lowry KE, Mills MM, Palmer MA, Balch WM, Bates NR, Benitez-Nelson CR, Brownlee E, Frey KE, Laney SR, Mathis J, Matsuoka A, Greg Mitchell B, Moore GWK, Reynolds RA, Sosik HM, Swift JH (2014) Phytoplankton blooms beneath the sea ice in the Chukchi sea. Deep Sea Research Part II: Topical Studies in Oceanography 105:1-16. doi:10.1016/j.dsr2.2014.03.018

Assmy P, Fernández-Méndez M, Duarte P, Meyer A, Randelhoff A, Mundy CJ, Olsen LM, Kauko HM, Bailey A, Chierici M (2017) Leads in Arctic pack ice enable early phytoplankton blooms below snow-covered sea ice. Scientific Reports 7:40850. doi:https://doi.org/10.1038/srep40850

Belt ST (2018) Source-specific biomarkers as proxies for Arctic and Antarctic sea ice. Organic geochemistry 125:277-298. doi:10.1016/j.orggeochem.2018.10.002

Belt ST, Brown TA, Rodriguez AN, Sanz PC, Tonkin A, Ingle R (2012) A reproducible method for the extraction, identification and quantification of the Arctic sea ice proxy IP_{25} from marine sediments. Analytical Methods 4. doi:10.1039/c2ay05728j

Belt ST, Massé G, Rowland SJ, Poulin M, Michel C, LeBlanc B (2007) A novel chemical fossil of palaeo sea ice: IP_{25}. Organic Geochemistry 38:16-27. doi:10.1016/j.orggeochem.2006.09.013

Belt ST, Müller J (2013) The Arctic sea ice biomarker IP_{25}: a review of current understanding, recommendations for future research and applications in palaeo sea ice reconstructions. Quaternary Science Reviews 79:9-25. doi:10.1016/j.quascirev.2012.12.001

Bluhm B, Iken K, Hardy SM, Sirenko B, Holladay B (2009) Community structure of epibenthic megafauna in the Chukchi Sea. Aquatic Biology 7:269-293. https://doi.org/10.3354/ab00198

Brown T, Alexander C, Yurkowski D, Ferguson S, Belt S (2014a) Identifying variable sea ice carbon contributions to the Arctic ecosystem: A case study using highly branched isoprenoid lipid biomarkers in Cumberland Sound ringed seals. Limnology and Oceanography 59:1581-1589. https://doi.org/10.4319/lo.2014.59.5.1581

Brown TA, Belt ST (2012) Closely linked sea ice-pelagic coupling in the Amundsen Gulf revealed by the sea ice diatom biomarker IP_{25}. Journal of Plankton Research 34:647-654. doi:10.1093/plankt/fbs045

Brown TA, Belt ST, Tatarek A, Mundy CJ (2014b) Source identification of the Arctic sea ice proxy IP_{25}. Nat Commun 5:4197. doi:10.1038/ncomms5197

Brown TA, Chrystal E, Ferguson SH, Yurkowski DJ, Watt C, Hussey NE, Kelley TC, Belt ST (2017) Coupled changes between the H-Print biomarker and $\delta^{15}N$ indicates a variable sea ice carbon contribution to the diet of Cumberland Sound beluga whales. Limnology and Oceanography 62:1606-1619. doi:10.1002/lno.10520

Brown TA, Galicia MP, Thiemann GW, Belt ST, Yurkowski DJ, Dyck MG (2018) High contributions of sea ice derived carbon in polar bear (Ursus maritimus) tissue. PLoS One 13:e0191631. doi:10.1371/journal.pone.0191631

Brown TA, Yurkowski DJ, Ferguson SH, Alexander C, Belt ST (2014c) H-Print: a new chemical fingerprinting approach for distinguishing primary production sources in Arctic ecosystems. Environmental Chemistry Letters 12:387-392. doi:10.1007/s10311-014-0459-1

Budge SM, Wooller MJ, Springer AM, Iverson SJ, McRoy CP, Divoky GJ (2008) Tracing carbon flow in an arctic marine food web using fatty acid-stable isotope analysis. Oecologia 157:117-129. doi:10.1007/s00442-008-1053-7

Cooper LW, Grebmeier JM (2018) Deposition patterns on the Chukchi shelf using radionuclide inventories in relation to surface sediment characteristics. Deep Sea Research Part II: Topical Studies in Oceanography 152:48-66. doi:10.1016/j.dsr2.2018.01.009

Cooper LW, Grebmeier JM, Larsen IL, Dolvin SS, Reed AJ (1998) Inventories and distribution of radiocaesium in Arctic marine sediments: Influence of biological and bhysical brocesses. Chemistry and Ecology 15:27-46. doi:10.1080/02757549808037619

Denisenko SG, Grebmeier JM, Cooper LW, Denisenko SG, Skvortsov VV (2015) Assessing bioresources and standing stock of zoobenthos (key species, high taxa, trophic groups) in the Chukchi Sea. Oceanography 28:146-157. doi:https://www.jstor.org/stable/24861907

Dezutter T, Lalande C, Dufresne C, Darnis G, Fortier L (2019) Mismatch between microalgae and herbivorous copepods due to the record sea ice minimum extent of 2012 and the late sea ice break-up of 2013 in the Beaufort Sea. Progress in Oceanography 173:66-77.

Divine LM, Bluhm BA, Mueter FJ, Iken K (2017) Diet analysis of Alaska Arctic snow crabs (Chionoecetes opilio) using stomach contents and δ13C and δ15N stable isotopes. Deep Sea Research Part II: Topical Studies in Oceanography 135:124-136. doi:https://doi.org/10.1016/j.dsr2.2015.11.009

Duffy-Anderson JT, Stabeno P, Andrews III AG, Cieciel K, Deary A, Farley E, Fugate C, Harpold C, Heintz R, Kimmel D (2019) Responses of the northern Bering Sea and southeastern Bering Sea pelagic ecosystems following record-breaking low winter sea ice. Geophysical Research Letters 46:9833-9842. https://doi.org/10.1029/2019GL083396

Dunton KH, Grebmeier JM, Trefry JH (2014) The benthic ecosystem of the northeastern Chukchi Sea: An overview of its unique biogeochemical and biological characteristics. Deep Sea Research Part II: Topical Studies in Oceanography 102:1-8. doi:10.1016/j.dsr2.2014.01.001

Encyclopedia of Life (2020) Accessed 07/28/2020. http://eol.org.

Falk-Petersen S, Sargent J, Henderson J, Hegseth E, Hop H, Okolodkov Y (1998) Lipids and fatty acids in ice algae and phytoplankton from the Marginal Ice Zone in the Barents Sea. Polar Biology 20:41-47. https://doi.org/10.1007/s003000050274

Feder HM, Naidu AS, Jewett SC, Hameedi JM, Johnson WR, Whitledge TE (1994) The northeastern Chukchi Sea: benthos-environmental interactions. Marine ecology progress series https://www.jstor.org/stable/24847621:171-190. doi:https://www.jstor.org/stable/24847621

Frey K, Comiso J, Cooper L, Grebmeier J, Stock LV (2018) Arctic ocean primary productivity: The response of marine algae to climate warming and sea ice decline. Arctic Report Card 2018, https://www.arctic.noaa.gov/Report-Card

Frey KE, Moore G, Cooper LW, Grebmeier JM (2015) Divergent patterns of recent sea ice cover across the Bering, Chukchi, and Beaufort seas of the Pacific Arctic Region. Progress in Oceanography 136:32-49. doi:10.1016/j.pocean.2015.05.009

Gibbs P (1977) On the status of Golfingia intermedia (Sipuncula). Journal of the Marine Biological Association of the United Kingdom 57:109-112. doi:https://doi.org/10.1017/S0025315400021275

Goethel CL, Grebmeier JM, Cooper LW (2019) Changes in abundance and biomass of the bivalve Macoma calcarea in the northern Bering Sea and the southeastern Chukchi Sea from 1998 to 2014, tracked through dynamic factor analysis models. Deep Sea Research Part II: Topical Studies in Oceanography 162:127-136. https://doi.org/10.1016/j.dsr2.2018.10.007

Gradinger R (2009) Sea-ice algae: Major contributors to primary production and algal biomass in the Chukchi and Beaufort Seas during May/June 2002. Deep Sea Research Part II: Topical Studies in Oceanography 56:1201-1212. doi:10.1016/j.dsr2.2008.10.016

Grebmeier JM, Bluhm BA, Cooper LW, Danielson SL, Arrigo KR, Blanchard AL, Clarke JT, Day RH, Frey KE, Gradinger RR (2015) Ecosystem characteristics and processes facilitating persistent macrobenthic biomass hotspots and associated benthivory in the Pacific Arctic. Progress in Oceanography 136:92-114. doi:10.1016/j.pocean.2015.05.006

Grebmeier JM, Cooper LW (1995) Influence of the St. Lawrence Island polynya upon the Bering Sea benthos. Journal of Geophysical Research: Oceans 100:4439-4460. doi:https://doi.org/10.1029/94JC02198

Grebmeier JM, Cooper LW (2019a) Benthic macroinfaunal samples collected from the Canadian Coast Guard Ship (CCGS) Sir Wilfrid Laurier, Northern Bering Sea to Chukchi Sea, 2015 10.18739/A28W3827B. Arctic Data Center

Grebmeier JM, Cooper LW (2019b) Surface sediment samples collected from the CCGS Sir Wilfrid Laurier 2018, Northern Bering Sea to Chukchi Sea. https://arcticdata.io/catalog/view/doi:10.18739/A2C824F2J

Grebmeier JM, Cooper LW (2019c) Surface sediment samples collected from the United States Coast Guard Cutter Healy (HLY1801), Northern Bering Sea to Chukchi Sea https://arcticdata.io/catalog/view/doi:10.18739/A2H12V769

Grebmeier JM, Cooper LW, Feder HM, Sirenko BI (2006a) Ecosystem dynamics of the Pacific-influenced Northern Bering and Chukchi Seas in the Amerasian Arctic. Progress in Oceanography 71:331-361. doi:10.1016/j.pocean.2006.10.001

Grebmeier JM, Frey KE, Cooper LW, Kędra M (2018) Trends in benthic macrofaunal populations, seasonal sea ice persistence, and bottom water temperatures in the Bering Strait region. Oceanography 31:136-151. https://www.jstor.org/stable/26542660

Grebmeier JM, Moore SE, Overland JE, Frey KE, Gradinger R (2010) Biological response to recent Pacific Arctic sea ice retreats. Eos, Transactions American Geophysical Union 91:161-162. doi:10.1029/2010EO180001

Grebmeier JM, Overland JE, Moore SE, Farley EV, Carmack EC, Cooper LW, Frey KE, Helle JH, McLaughlin FA, McNutt SL (2006b) A Major Ecosystem Shift in the Northern Bering Sea. Science 311:1461-1464. doi:10.1126/science.1121365

Hill V, Ardyna M, Lee SH, Varela DE (2018) Decadal trends in phytoplankton production in the Pacific Arctic Region from 1950 to 2012. Deep Sea Research Part II: Topical Studies in Oceanography 152:82-94. doi:10.1016/j.dsr2.2016.12.015

Iken K, Bluhm B, Dunton K (2010) Benthic food-web structure under differing water mass properties in the southern Chukchi Sea. Deep Sea Research Part II: Topical Studies in Oceanography 57:71-85. https://doi.org/10.1016/j.dsr2.2009.08.007

Jansen JM, Pronker AE, Kube S, Sokolowski A, Sola JC, Marquiegui MA, Schiedek D, Bonga SW, Wolowicz M, Hummel H (2007) Geographic and seasonal patterns and limits on the adaptive response to temperature of European Mytilus spp. and Macoma balthica populations. Oecologia 154:23-34. doi:https://doi.org/10.1007/s00442-007-0808-x

Jay CV, Grebmeier JM, Fischbach AS, McDonald TL, Cooper LW, Hornsby F (2014) Pacific walrus (Odobenus rosmarus divergens) resource selection in the Northern Bering Sea. PLoS One 9:e93035. doi:10.1371/journal.pone.0093035

Kędra M, Cooper LW, Zhang M, Biasatti D, Grebmeier JM (2019) Benthic trophic sensitivity to on-going changes in Pacific Arctic seasonal sea ice cover – Insights from the nitrogen isotopic composition of amino acids. Deep Sea Research Part II: Topical Studies in Oceanography 162:137-151. doi:10.1016/j.dsr2.2019.01.002

Kędra M, Grebmeier JM, Cooper LW (2018) Sipunculan fauna in the Pacific Arctic region: a significant component of benthic infaunal communities. Polar Biology 41:163-174. https://doi.org/10.1007/s00300-017-2179-z

Kędra M, Moritz C, Choy ES, David C, Degen R, Duerksen S, Ellingsen I, Górska B, Grebmeier JM, Kirievskaya D, van Oevelen D, Piwosz K, Samuelsen A, Węsławski JM (2015) Status and trends in the structure of Arctic benthic food webs. Polar Research 34. doi:10.3402/polar.v34.23775

Koch CW, Cooper LW, Lalande C, Brown TA, Frey KE, Grebmeier JM (2020) Seasonal and latitudinal variations in sea ice algae deposition in the Northern Bering and Chukchi Seas determined by algal biomarkers. PLoS One 15:e0231178., https://doi.org/10.1371/journal.pone.0231178

Kohlbach D, Ferguson SH, Brown TA, Michel C (2019) Landfast sea ice-benthic coupling during spring and potential impacts of system changes on food web dynamics in Eclipse Sound, Canadian Arctic. Marine Ecology Progress Series 627:33-48. doi:https://doi.org/10.3354/meps13071

Kohlbach D, Graeve M, A. Lange B, David C, Peeken I, Flores H (2016) The importance of ice algae-produced carbon in the central Arctic Ocean ecosystem: Food web relationships revealed by lipid and stable isotope analyses. Limnology and Oceanography 61:2027-2044. doi:10.1002/lno.10351

Kohlbach D, Graeve M, Lange BA, David C, Schaafsma FL, van Franeker JA, Vortkamp M, Brandt A, Flores H (2018) Dependency of Antarctic zooplankton species on ice algae-produced carbon suggests a sea ice-driven pelagic ecosystem during winter. Global change biology 24:4667-4681. doi:https://doi.org/10.1111/gcb.14392

Kremer A, Stein R, Fahl K, Ji Z, Yang Z, Wiers S, Matthiessen J, Forwick M, Löwemark L, O'Regan M (2018) Changes in sea ice cover and ice sheet extent at the Yermak Plateau during the last 160 ka–Reconstructions from biomarker records. Quaternary Science Reviews 182:93-108. doi:https://doi.org/10.1016/j.quascirev.2017.12.016

Legendre L, Ackley SF, Dieckmann GS, Gulliksen B, Horner R, Hoshiai T, Melnikov IA, Reeburgh WS, Spindler M, Sullivan CW (1992) Ecology of sea ice biota. Polar biology 12:429-444. doi:10.1007/BF00243114

Lepore K, Moran S, Smith J (2009) ^{210}Pb as a tracer of shelf–basin transport and sediment focusing in the Chukchi Sea. Deep Sea Research Part II: Topical Studies in Oceanography 56:1305-1315. https://doi.org/10.1016/j.dsr2.2008.10.021

Leu E, Mundy CJ, Assmy P, Campbell K, Gabrielsen TM, Gosselin M, Juul-Pedersen T, Gradinger R (2015) Arctic spring awakening – Steering principles behind the phenology of vernal ice algal blooms. Progress in Oceanography 139:151-170. doi:10.1016/j.pocean.2015.07.012

Leu E, Søreide JE, Hessen DO, Falk-Petersen S, Berge J (2011) Consequences of changing sea-ice cover for primary and secondary producers in the European Arctic shelf seas: Timing, quantity, and quality. Progress in Oceanography 90:18-32. doi:10.1016/j.pocean.2011.02.004

Lewis K, van Dijken G, Arrigo K (2020) Changes in phytoplankton concentration now drive increased Arctic Ocean primary production. Science 369:198-202. doi:10.1126/science.aay8380

Li WK, McLaughlin FA, Lovejoy C, Carmack EC (2009) Smallest algae thrive as the Arctic Ocean freshens. Science 326:539-539. doi:10.1126/science.1179798

Limoges A, Massé G, Weckström K, Poulin M, Ellegaard M, Heikkilä M, Geilfus N-X, Sejr MK, Rysgaard S, Ribeiro S (2018) Spring succession and vertical export of diatoms and IP_{25} in a seasonally ice-covered high Arctic fjord. Frontiers in Earth Science 6. doi:10.3389/feart.2018.00226

Macdonald TA, Burd B, Macdonald V, Van Roodselaar A (2010) Taxonomic and feeding guild classification for the marine benthic macroinvertebrates of the Strait of Georgia, British Columbia. Fisheries and Oceans Canada= Pêches et océans Canada

Mäkelä A, Witte U, Archambault P (2017) Ice algae versus phytoplankton: resource utilization by Arctic deep sea macroinfauna revealed through isotope labelling experiments. Marine Ecology Progress Series 572:1-18. doi:10.3354/meps12157

McMahon KW, Ambrose Jr WG, Johnson BJ, Sun M-Y, Lopez GR, Clough LM, Carroll ML (2006) Benthic community response to ice algae and phytoplankton in Ny Ålesund, Svalbard. Marine Ecology Progress Series 310:1-14. doi:10.3354/meps310001

McTigue ND, Dunton KH (2014) Trophodynamics and organic matter assimilation pathways in the northeast Chukchi Sea, Alaska. Deep Sea Research Part II: Topical Studies in Oceanography 102:84-96. doi:10.1016/j.dsr2.2013.07.016

Mincks SL, Smith CR, DeMaster DJ (2005) Persistence of labile organic matter and microbial biomass in Antarctic shelf sediments: evidence of a sediment 'food bank'. Marine Ecology Progress Series 300:3-19. doi:10.3354/meps300003

Mohan SD, Connelly TL, Harris CM, Dunton KH, McClelland JW (2016) Seasonal trophic linkages in Arctic marine invertebrates assessed via fatty acids and compound-specific stable isotopes. Ecosphere 7. https://doi.org/10.1002/ecs2.1429

Moore SE, Grebmeier JM (2018) The Distributed Biological Observatory. Arctic 71:1-7. doi:https://doi.org/10.14430/arctic4606

Moore SE, Huntington HP (2008) Arctic marine mammals and climate change: impacts and resilience. Ecological Applications 18:S157-S165. https://doi.org/10.1890/06-0571.1
Moore SE, Stabeno PJ (2015) Synthesis of Arctic Research (SOAR) in marine ecosystems of the Pacific Arctic. Progress in Oceanography 136:1-11. doi:10.1016/j.pocean.2015.05.017
Moore SE, Stabeno PJ, Grebmeier JM, Okkonen SR (2018) The Arctic Marine Pulses Model: linking annual oceanographic processes to contiguous ecological domains in the Pacific Arctic. Deep Sea Research Part II: Topical Studies in Oceanography 152:8-21. doi:10.1016/j.dsr2.2016.10.011
Müller J, Stein R (2014) High-resolution record of late glacial and deglacial sea ice changes in Fram Strait corroborates ice–ocean interactions during abrupt climate shifts. Earth and Planetary Science Letters 403:446-455. doi:10.1016/j.epsl.2014.07.016
North CA, Lovvorn JR, Kolts JM, Brooks ML, Cooper LW, Grebmeier JM (2014) Deposit-feeder diets in the Bering Sea: potential effects of climatic loss of sea ice-related microalgal blooms. Ecological applications 24:1525-1542. https://doi.org/10.1890/13-0486.1
Overland JE, Stabeno PJ (2004) Is the climate of the Bering Sea warming and affecting the ecosystem? Eos, Transactions American Geophysical Union 85:309-312. https://doi.org/10.1029/2004EO330001
Pickart RS, Nobre C, Lin P, Arrigo KR, Ashjian CJ, Berchok C, Cooper LW, Grebmeier JM, Hartwell I, He J (2019) Seasonal to mesoscale variability of water masses and atmospheric conditions in Barrow Canyon, Chukchi Sea. Deep Sea Research Part II: Topical Studies in Oceanography 162:32-49. https://doi.org/10.1016/j.dsr2.2019.02.003
Pickart RS, Weingartner TJ, Pratt LJ, Zimmermann S, Torres DJ (2005) Flow of winter-transformed Pacific water into the Western Arctic. Deep Sea Research Part II: Topical Studies in Oceanography 52:3175-3198. https://doi.org/10.1016/j.dsr2.2005.10.009
Pirtle-Levy R, Grebmeier JM, Cooper LW, Larsen IL (2009) Chlorophyll a in Arctic sediments implies long persistence of algal pigments. Deep Sea Research Part II: Topical Studies in Oceanography 56:1326-1338. doi:10.1016/j.dsr2.2008.10.022
Pisareva MN, Pickart RS, Iken K, Ershova EA, Grebmeier JM, Cooper LW, Bluhm BA, Nobre C, Hopcroft RR, Hu H, Wang J, Ashjian CJ, Kosobokova KN, Whitledge TE (2015) The relationship between patterns of benthic fauna and zooplankton in the Chukchi Sea and physical forcing. Oceanography 28:68-83. www.jstor.org/stable/24861902
R Core Team (2017) R: A language and environment for statistical computing. R Foundation for Statistical Computing. https://www.R-project.org R Foundation for Statistical Computing Vienna, Austria
Riedel A, Michel C, Gosselin M (2006) Seasonal study of sea-ice exopolymeric substances on the Mackenzie shelf: implications for transport of sea-ice bacteria and algae. Aquatic microbial ecology 45:195-206.
Schollmeier T, Oliveira A, Wooller M, Iken K (2018) Tracing sea ice algae into various benthic feeding types on the Chukchi Sea shelf. Polar Biology 41:207-224. https://doi.org/10.1007/s00300-017-2182-4
Selz V, Laney S, Arnsten AE, Lewis KM, Lowry KE, Joy-Warren HL, Mills MM, van Dijken GL, Arrigo KR (2018) Ice algal communities in the Chukchi and Beaufort Seas in spring and early summer: Composition, distribution, and coupling with phytoplankton assemblages. Limnology and Oceanography 63:1109-1133. doi:10.1002/lno.10757
Serreze MC, Meier WN (2018) The Arctic's sea ice cover: trends, variability, predictability, and comparisons to the Antarctic. Annals of the New York Academy of Sciences 10.1111/nyas.13856 doi:10.1111/nyas.13856
Sheffield G, Grebmeier JM (2009) Pacific walrus (Odobenus rosmarus divergens): Differential prey digestion and diet. Marine Mammal Science 25:761-777. doi:10.1111/j.1748-7692.2009.00316.x
Søreide JE, Leu EV, Berge J, Graeve M, Falk-Petersen S (2010) Timing of blooms, algal food quality and Calanus glacialis reproduction and growth in a changing Arctic. Global change biology 16:3154-3163. doi:https://doi.org/10.1111/j.1365-2486.2010.02175.x

Stabeno PJ, Bell SW (2019) Extreme conditions in the Bering Sea (2017–2018): Record-breaking low sea-ice extent. Geophysical Research Letters 46:8952-8959. https://doi.org/10.1029/2019GL083816

Stein R, Fahl K, Gierz P, Niessen F, Lohmann G (2017) Arctic Ocean sea ice cover during the penultimate glacial and the last interglacial. Nature communications 8:1-13. doi:https://doi.org/10.1038/s41467-017-00552-1

Stein R, Fahl K, Schreck M, Knorr G, Niessen F, Forwick M, Gebhardt C, Jensen L, Kaminski M, Kopf A (2016) Evidence for ice-free summers in the late Miocene central Arctic Ocean. Nature Communications 7:1-13. doi:https://doi.org/10.1038/ncomms11148

Sun M-Y, Clough LM, Carroll ML, Dai J, Ambrose Jr WG, Lopez GR (2009) Different responses of two common Arctic macrobenthic species (Macoma balthica and Monoporeia affinis) to phytoplankton and ice algae: Will climate change impacts be species specific? Journal of Experimental Marine Biology and Ecology 376:110-121. https://doi.org/10.1016/j.jembe.2009.06.018

Szymanski A, Gradinger R (2016) The diversity, abundance and fate of ice algae and phytoplankton in the Bering Sea. Polar Biology 39:309-325. doi:10.1007/s00300-015-1783-z

Thoman RL, Bhatt US, Bieniek PA, Brettschneider BR, Brubaker M, Danielson SL, Labe Z, Lader R, Meier WN, Sheffield G (2020) The record low Bering Sea ice extent in 2018: Context, impacts, and an assessment of the role of anthropogenic climate change. Bulletin of the American Meteorological Society 101:S53-S58.

Thyrring J, Rysgaard S, Blicher ME, Sejr MK (2015) Metabolic cold adaptation and aerobic performance of blue mussels (Mytilus edulis) along a temperature gradient into the High Arctic region. Marine Biology 162:235-243. doi:https://doi.org/10.1007/s00227-014-2575-7

Tibshirani R, Walther G, Hastie T (2001) Estimating the number of clusters in a data set via the gap statistic. Journal of the Royal Statistical Society: Series B (Statistical Methodology) 63:411-423. doi:https://doi.org/10.1111/1467-9868.00293

Tremblay J-E, Michel C, Hobson KA, Gosselin M, Price NM (2006) Bloom dynamics in early opening waters of the Arctic Ocean. Limnology and Oceanography 51:900-912. https://doi.org/10.4319/lo.2006.51.2.0900

Volkman JK, Barrett SM, Dunstan GA (1994) C25 and C30 highly branched isoprenoid alkenes in laboratory cultures of two marine diatoms. Organic Geochemistry 21:407-414. doi:10.1016/0146-6380(94)90202-X

Waga H, Hirawake T, Grebmeier JM (2020) Recent change in benthic macrofaunal community composition in relation to physical forcing in the Pacific Arctic. Polar Biology, https://doi.org/10.1007/s00300-020-02632-3:1-10.

Wang SW, Budge SM, Gradinger RR, Iken K, Wooller MJ (2014) Fatty acid and stable isotope characteristics of sea ice and pelagic particulate organic matter in the Bering Sea: tools for estimating sea ice algal contribution to Arctic food web production. Oecologia 174:699-712. https://doi.org/10.1007/s00442-013-2832-3

Weingartner T, Fang Y-C, Winsor P, Dobbins E, Potter R, Statscewich H, Mudge T, Irving B, Sousa L, Borg K (2017) The summer hydrographic structure of the Hanna Shoal region on the northeastern Chukchi Sea shelf: 2011–2013. Deep Sea Research Part II: Topical Studies in Oceanography 144:6-20. doi:10.1016/j.dsr2.2017.08.006

8. Tables

Sampling date (yyyy-mm-dd)	Station ID	Latitude (°N)	Longitude (°W)	Sampling depth (m)	Cruise collected
2018-06-11	DBO 2.4	64.964	-169.889	46	SKQ2018
2018-06-11	Diomede	65.753	-168.871	30	SKQ2018
2018-06-14	DBO 3.8	67.670	-168.951	51	SKQ2018
2018-06-15	DBO 3.3	68.189	-167.308	49	SKQ2018
2018-06-12	CNL3	66.510	-168.959	56	SKQ2018
2018-07-16	SLIP1	62.009	-175.063	80	SWL18
2018-07-16	SLIP2	62.049	-175.206	82	SWL18
2018-07-16	SLIP3	62.391	-174.569	72	SWL18
2018-07-17	SLIP5	62.558	-173.558	66	SWL18
2018-07-18	UTBS2	64.681	-169.100	45	SWL18
2018-07-18	UTBS1	64.992	-169.140	49	SWL18
2018-07-18	DBO2.7	65.000	-168.220	46	SWL18
2018-07-19	UTN1	66.709	-168.398	35	SWL18
2018-07-19	UTN2	67.050	-168.728	46	SWL18
2018-07-19	UTN3	67.331	-168.905	50	SWL18
2018-07-20	UTN4	67.500	-168.909	50	SWL18
2018-07-20	SEC4	68.013	-167.866	54	SWL18
2018-07-21	SEC1	67.672	-168.930	50	SWL18
2018-07-21	UTN6	67.740	-168.441	51	SWL18
2018-07-21	SEC2	67.784	-168.602	50	SWL18
2018-07-21	SEC3	67.899	-168.236	59	SWL18
2018-07-21	UTN7	68.000	-168.929	58	SWL18
2018-07-21	SEC5	68.128	-167.493	51	SWL18
2018-07-22	DBO4.4	71.588	-161.401	49	SWL18
2018-07-22	DBO4.5	71.610	-161.615	44	SWL18
2018-07-23	DBO4.3	71.454	-161.036	49	SWL18
2018-08-08	UTBS2A	64.671	-168.234	39	HLY18-01
2018-08-08	UTBS1	64.991	-169.146	49	HLY18-01
2018-08-09	UTBS5	64.672	-169.926	48	HLY18-01
2018-08-09	T2	67.164	-168.664	47	HLY18-01
2018-08-10	SEC4/DBO3.5	68.015	-167.880	51	HLY18-01
2018-08-10	SEC5/DBO3.4	68.136	-167.492	48	HLY18-01
2018-08-11	SEC1/DBO3.8	67.677	-168.957	51	HLY18-01
2018-08-11	SEC2/DBO3.7	68.246	-167.126	51	HLY18-01
2018-08-12	IC-10	71.705	-165.603	43	HLY18-01
2018-08-13	IC-6	71.195	-164.202	45	HLY18-01
2018-08-13	IC-8	71.449	-164.919	43	HLY18-01
2018-08-13	IC-9	71.601	-165.304	43	HLY18-01
2018-08-14	IC-1	70.580	-162.491	39	HLY18-01
2018-08-14	IC-2	70.717	-162.857	43	HLY18-01

2018-08-14	IC-3	70.849	-163.187	45	HLY18-01
2018-08-15	DBO4.3	71.351	-161.396	49	HLY18-01
2018-08-15	DBO4.4	71.481	-161.505	49	HLY18-01
2018-08-15	DBO4.5	71.610	-161.615	47	HLY18-01
2018-08-17	DBO5.1	71.247	-157.135	45	HLY18-01
2018-08-17	DBO5.2	71.289	-157.221	56	HLY18-01
2018-08-17	DBO5.4	71.373	-157.380	116	HLY18-01
2018-08-17	DBO5.5	71.410	-157.450	131	HLY18-01
2018-08-17	DBO5.6	71.454	-157.553	120	HLY18-01
2018-08-17	DBO5.7	71.495	-157.627	96	HLY18-01
2018-08-17	DBO5.8	71.536	-157.711	75	HLY18-01
2018-08-17	DBO5.10	71.626	-157.901	64	HLY18-01

Table 1 – Station summary for the ASGARD cruise SKQ2018 and the Distributed Biological Observatory (DBO) cruises SWL18 and HLY18-01.

Species	Sample size (n)	Feeding Strategy	SKQ (trawls)	SWL (grabs)	HLY (grabs)	DBO Sample Regions
Holothuroidea						
Amphideima sp.	1	SUS[a]	X			2
Chiridota sp.	1	SDF[a]	X			2
Ocnus glacialis	2	SUS[b]	X			3
Myriotrochus sp.	1	SUS[a]		X		3
Ascidacea (Tunicata)						
Styela rustica	4	SUS[b]	X	X	X	2, 3, 5
Pelonaia corrugata	2	SUS[b]	X			2, 3
Boltenia ovifera	2	SUS[b]	X			2
Boltenia echinata	3	SUS[b]	X			3
Chelyosoma macleayanum	3	SUS[b]	X			3
Gastropoda						
Neptunea heros	3	P/S[b]	X			2
Neptunea communis	1	P/S[b]	X			2
Buccinum scalariforme	2	P/S[b]	X			2
Buccinum polare	2	P/S[b]	X			3
Cryptonatica affinis	5	P/S[b]	X			2, 3
Bivalvia						
Serripes lamperosii	7	SUS [a,b]	X	X	X	3

Macoma calcarea	37	SUS/SDF[c]	X	X	X	ALL
Ennucula tenuis	18	SSDF[c]		X	X	ALL
Nuculana pernicula	2	SSDF[b]		X		3, 4
Astarte borealis	4	SUS[c]		X	X	IC, 4, 5
Yoldia hyperborea	11	SSDF[c]		X	X	3, IC, 4, 5
Mya truncata	2	SUS[b]		X		3
Mya sp.	1	SUS[b]		X		3
Musculus sp.	2	SUS[b]		X	X	IC, 4
Hiatella arctica	1	SUS[b]	X			3
Pandora sp.	1	SUS[b]			X	IC
Lysianassidae unidentified sp.	1	P/S[b]			X	IC
Nutricola sp.	2	SUS[b]			X	IC, 5
Polychatea						
Gattyana ciliata	1	SSDF[b]	X			2
Gattyana sp.	1	SSDF[b]	X			3
Eunoe sp.	1	P/S[b]	X			3
Nephtys sp.	8	P/S[b]		X	X	2, 3, 5
Pectinaria hyperborea	12	SSDF[b]		X	X	1, 3, 4, IC, 5
Maldane sp.	18	SSDF[b,c]		X	X	ALL
Echiurus echiurus	3	SDF[a]	X			3
Lumbrineris sp.	1	SSDF[b]				IC
Sipuncula						
Golfingia margaritacea	6	SDF[d]			X	3, IC, 5
Ophiuroidea						
Ophiura sarsii	3	SDF[b]		X		1, 4
Gorgonocephalus sp.	1	P/S[b]			X	5
Malacastroca (Decapoda)						
Pandalus eous	1	P/S[b]		X		1
Pagurus trigonocheirus	1	P/S[b]	X			2
Chionoecetes opilio	2	P/S[e]		X		1, 3
Malacastroca (Amphipoda)						
Isaeidae sp.	2	SDF[b]		X		2, 3
Ampeliscia sp.	11	SUS[b]		X	X	1,2,4,5
Asteroidea						
Henricia sp.	1	P/S[b]			X	4
Anthozoa						
Gersemia rubiformis	1	SUS[b]	X			2

[a]Encyclopedia of Life 2020

[b]MacDonald et al. 2010
[c]Denisenko et al. 2015
[d]Kędra et al. 2018
[e]Divine et al. 2017

Table 2. Summary of taxa collected in 2018 for HBI biomarkers with assigned feeding strategy, cruise (SKQ=SKQ2018, SWL=SWL18, HLY=HLY18-01) and collection method, along with the Distributed Biological Observatory (DBO) sample region (see Fig. 1). Feeding strategies were classified as **SUS** (suspension), **SUS/SDF** (suspension/surface deposit), **SDF** (surface deposit), **SSDF** (subsurface deposit), and **P/S** (predator/scavenger). Sample size indicates number of stations with the species analyzed.

Group	Factor	DF	*SS*	*MS*	F	p-adj
DBO 1	Feeding strategy	4	113.4	28.36	0.70	0.612
	Residuals	9	365.4	40.60		
DBO 2	Feeding strategy	4	302.7	75.66	1.51	0.23
	Residuals	25	1252.7	50.11		
DBO 3	Feeding strategy	4	267.9	66.98	2.72	0.0358*
	Residuals	73	1796.5	24.61		
Icy Cape	Feeding strategy	4	2898.0	724.60	3.08	0.049*
	Residuals	15	3534.0	235.60		
DBO 4	Feeding strategy	4	2657.0	664.30	5.46	0.002**
	Residuals	27	3288.0	121.80		
DBO 5	Feeding strategy	4	4645.0	1161.30	3.47	0.036*
	Residuals	14	4680.0	334.30		
Cluster 1	Feeding strategy	4	847.8	211.95	2.36	0.0818
	Residuals	24	2154.0	89.75		
Cluster 2	Feeding strategy	4	1814.0	453.40	3.93	0.009**
	Residuals	39	4501.0	115.40		
Cluster 3	Feeding strategy	4	521.5	130.40	7.76	<0.001***
	Residuals	70	1176.2	16.80		

Table 3. ANOVA results for H-Print for each of the Distributed Biological Observatory (DBO) regions and clusters. Significant p-values are denoted as <0.05 (*), <0.01 (**) and <0.001 (***).

1

	Cluster Composition								
	DBO Region		Feeding Strategy		Dominant Taxa		Mean sediment H-print (%)	Mean sea ice carbon (iPOC %)	Mean Sea Ice Persistence (days)
Cluster 1	1	-	Suspension (SUS)	38%	Bivalvia	62%	mixed composition		
(n=29)	2	-	Subsurface deposit (SSDF)	28%	Polychaeta	21%	42 ± 11	17 ± 10	205 ± 35
	3	7%	Suspension/Surface deposit (SUS/SDF)	17%					
	IC	52%	Surface deposit (SDF)	3%					
	4	14%	Predator/Scavenger (PS)	14%					
	5	28%							
Cluster 2	1	-	Suspension (SUS)	7%	Bivalvia	52%	sympagic		
(n=44)	2	-	Subsurface deposit (SSDF)	57%	Polychaeta	25%	29 ± 7	53 ± 12	227 ± 18
	3	-	Suspension/Surface deposit (SUS/SDF)	18%	Sipuncula	9%			
	IC	6%	Surface deposit (SDF)	14%					
	4	66%	Predator/Scavenger (PS)	5%					
	5	25%							
Cluster 3	1	19%	Suspension (SUS)	27%	Bivalvia	52%	pelagic		
(n=75)	2	19%	Subsurface deposit (SSDF)	35%	Polychaeta	27%	80 ± 5	5 ± 5	111 ± 55
	3	63%	Suspension/Surface deposit (SUS/SDF)	27%	Ampeliscidae	13%			
	IC	-	Surface deposit (SDF)	3%					
	4	-	Predator/Scavenger (PS)	9%					
	5	-							

2

Table 4. Summary parameters for the k-means clustering analysis including the cluster composition by DBO region, feeding strategy and dominant taxa, mean sediment H-Print (%), mean macrofaunal tissue sea ice organic carbon (iPOC %), and mean sea ice persistence.

9. Figures

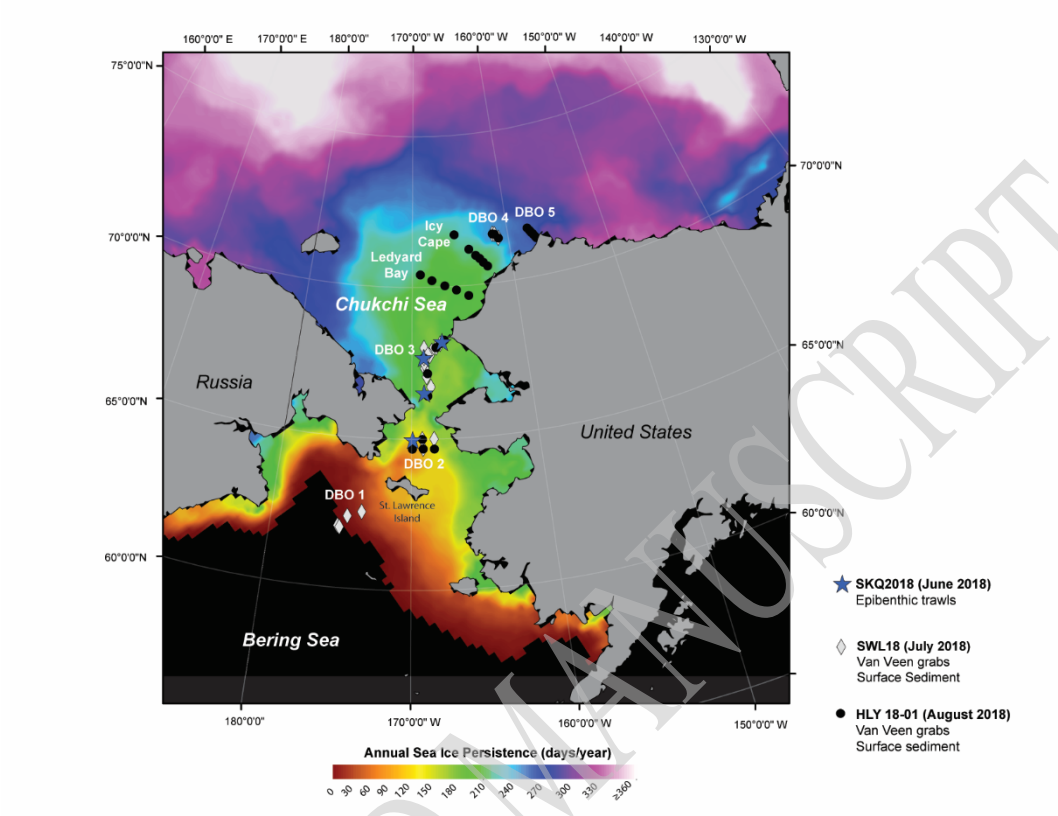

Figure 1 – Sampling locations in the northern Bering and Chukchi Seas in June (ASGARD, SKQ2018, blue stars), July (DBO, SWL18, black dots), and August (DBO, HLY18-01, gray diamonds) 2018 with corresponding sampling methods. Sea ice persistence is shown as days of sea ice cover (i.e., >15% concentration) per year, which was defined as the sea ice period from 14 September 2017 through 15 September 2018. The areas in black were ice-free throughout the entire year-long period.

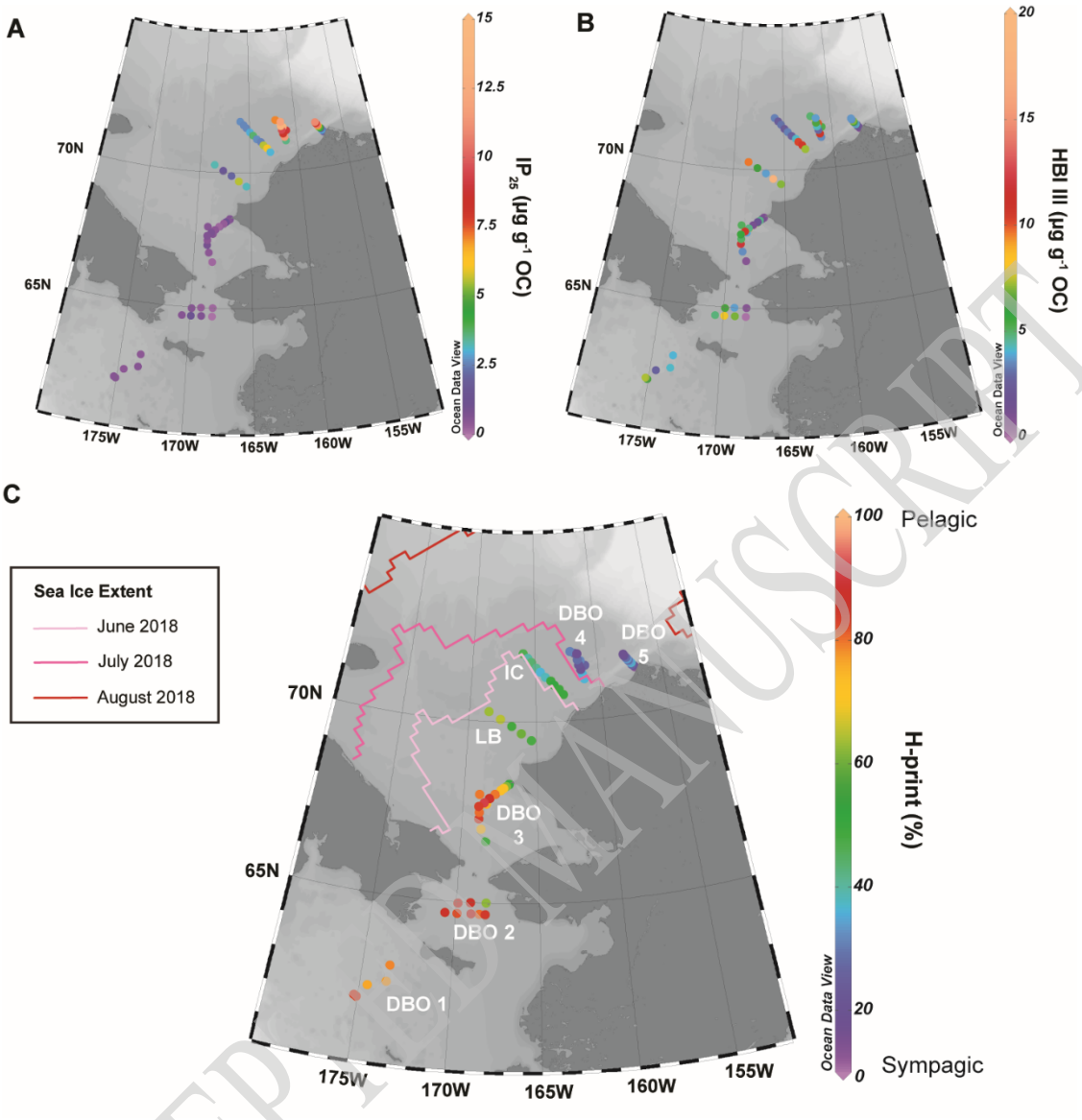

Figure 2 – Highly branched isoprenoid biomarker analysis from surface sediments collected in July (SWL18) and August (HLY18-01) in the northern Bering and Chukchi Seas. Sampling stations are shown as grey circles. **(A)** Distribution of the sea ice proxy IP_{25} (µg g OC^{-1}). **(B)** distribution of the pelagic HBI marker, HBI III (µg g OC^{-1}). **(C)** The H-Print (%) determined from sympagic (IP_{25} and HBI II) and pelagic (HBI III) biomarker proportions. Sample regions included DBO 1, DBO 2, DBO 3, Ledyard Bay (LB), Icy Cape (IC), DBO 4 and DBO 5. Note:

LB was only sampled for sediments and not macrofauna. The mean monthly sea ice extent is shown for June, July and August 2018.

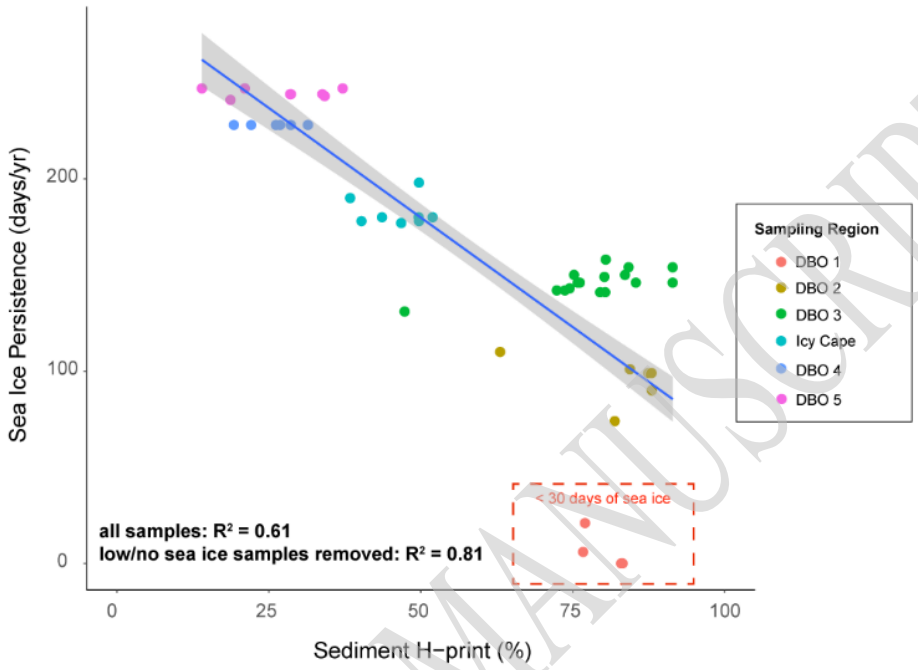

Figure 3 – Linear regression with 95% confidence interval (shaded region) of sea ice persistence (days/year) and sediment H-Print (%). Colors indicate the DBO sampling regions. The no/low sea ice stations were deemed outliers and the corresponding r^2 values with and without these outliers are shown.

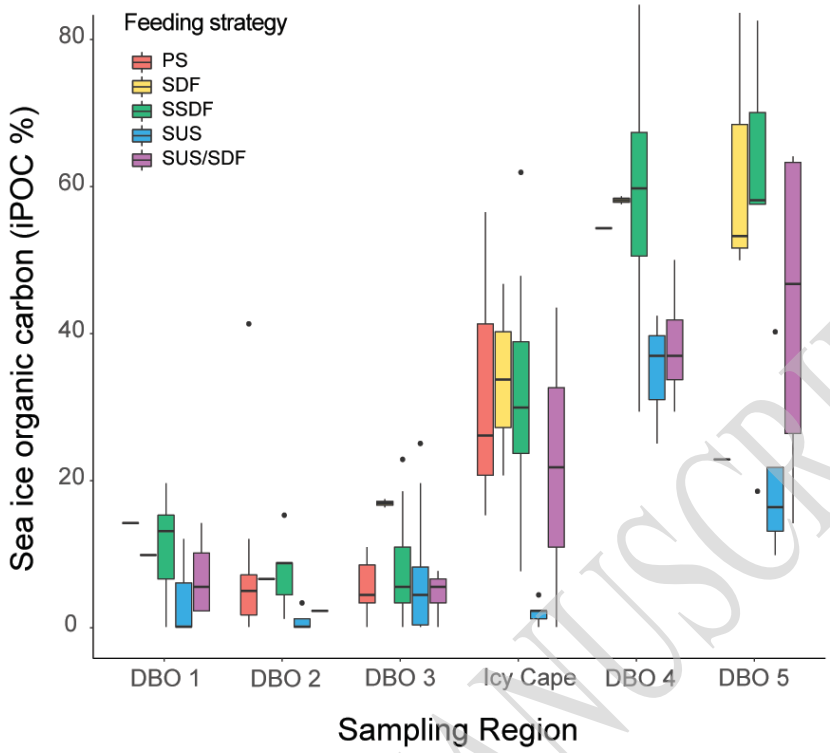

Figure 4 – Sea ice organic carbon (iPOC %) by feeding strategy across the Distributed Biological Observatory (DBO) sampling regions in 2018. Feeding strategies include: predator/scavengers (P/S), suspension (SUS), surface deposit (SDF), subsurface deposit (SSDF), and suspension/surface deposit feeders (SUS/SDF). Sample regions from south to north included DBO 1, DBO 2, DBO 3, Icy Cape, DBO 4 and DBO 5. The boxes indicate the interquartile range from the first to third quartiles, with the median shown as the line within each box. The minimum and maximum are indicated by the lines and outliers are shown as individual points.

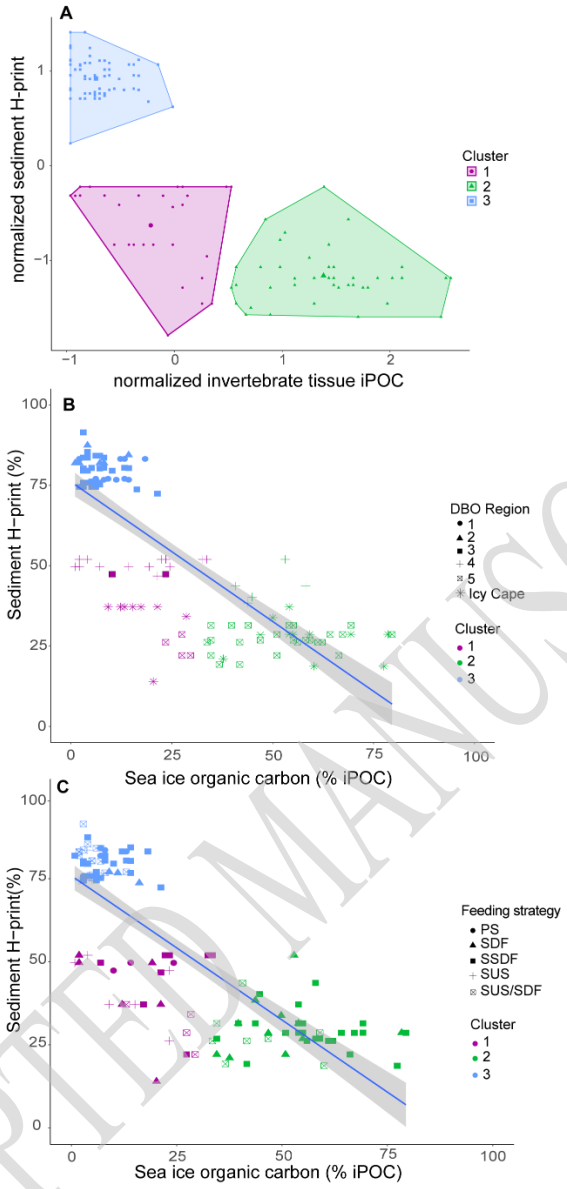

Figure 5 – Results of the k-means clustering analysis between macrofaunal tissue and the sediment the organisms were collected from **(A)** normalized sediment H-print and macrofauna tissue iPOC values grouped into the optimal number of clusters (3), **(B)** sediment H-Print (%) and macrofaunal tissue iPOC (%) with symbols represented by DBO sampling region and color represent cluster number. The linear regression is shown with a 95% confidence interval. **(C)** sediment H-Print (%) and invertebrate tissue iPOC (%) with symbols represented by feeding

strategy and color represent cluster number. The linear regression is shown with a 95% confidence interval. Feeding strategies as defined in Table 2.

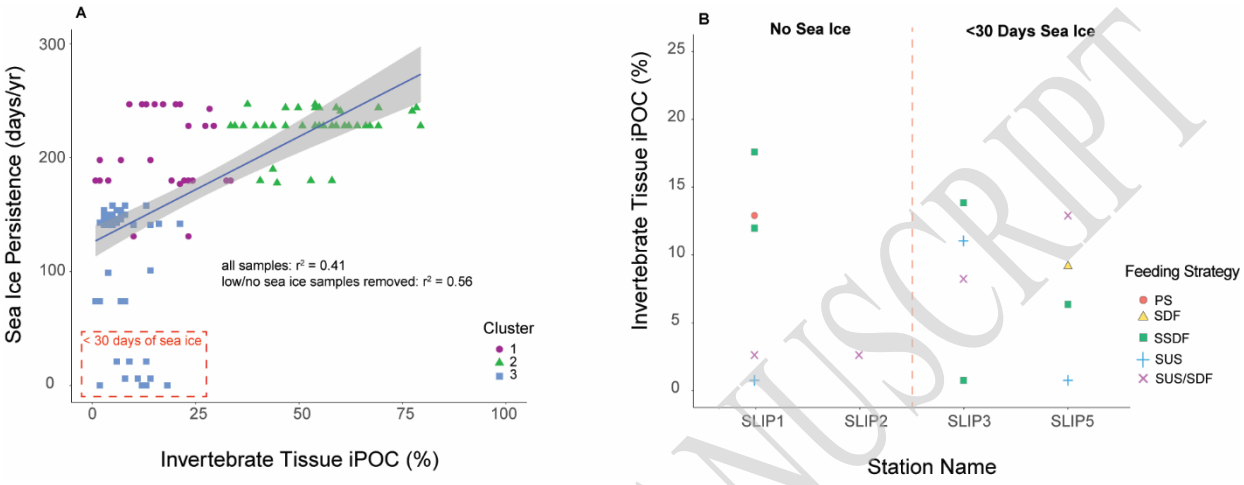

Figure 6 – (A) Linear regression of sea ice persistence and macrofauna sea ice organic carbon (iPOC %). Clusters are represented by corresponding shape/color. The samples that were deemed outliers due to low sea ice persistence or no sea ice cover in 2018 are enclosed in the dashed-red box. The linear regression is shown with a 95% confidence interval. **(B)** The macrofaunal tissue iPOC (%) from the no/low sea ice group by station in the DBO 1/St. Lawrence Island Polynya (SLIP) region. Symbols and corresponding colors represent feeding strategies of individual samples at these locations.

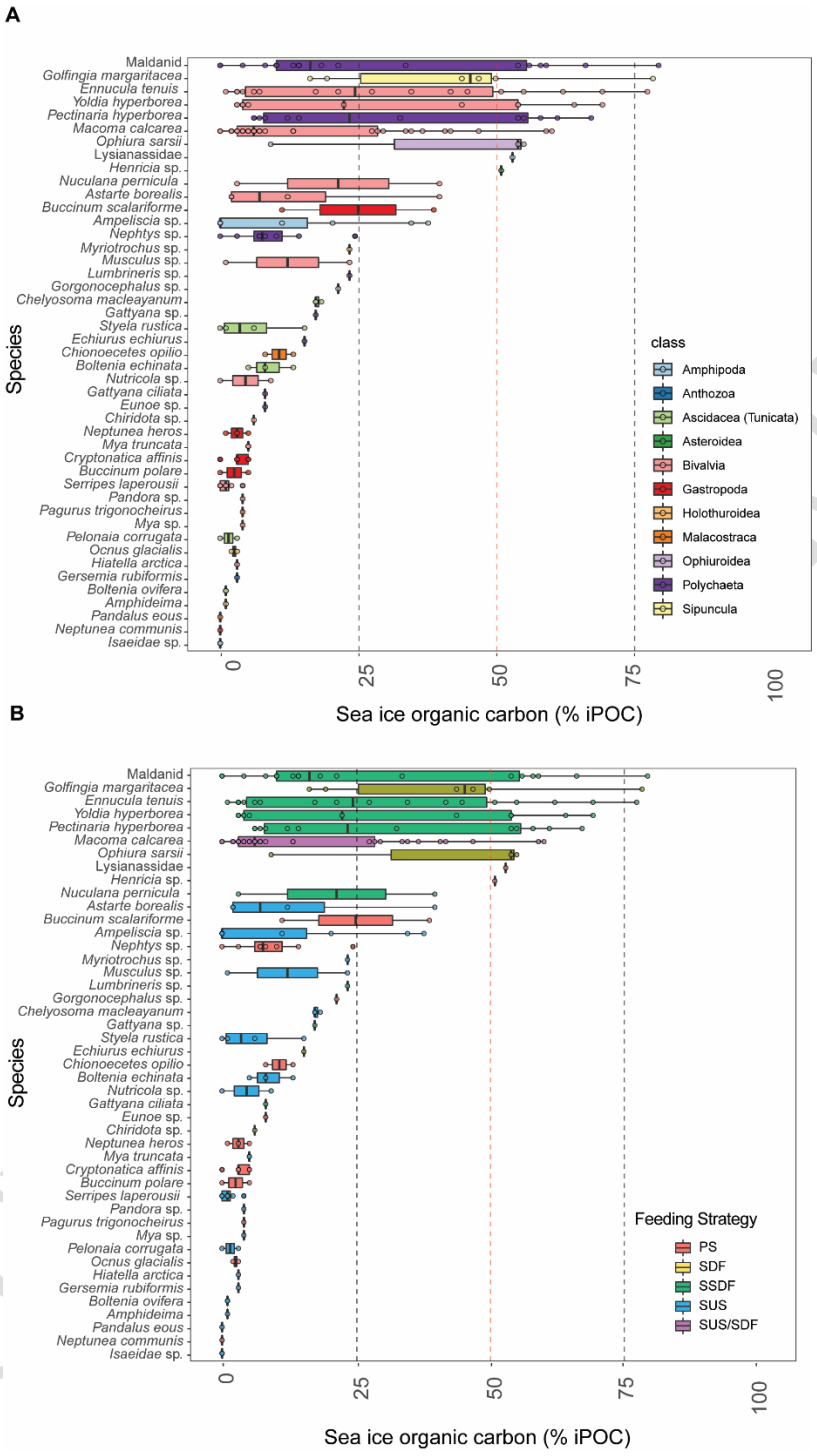

Figure 7 – Sea ice organic carbon (% iPOC) composition by species and shown by **(A)** major taxa and **(B)** feeding strategy. See Fig. 3 for boxplot descriptions and Table 2 for feeding strategies. Shaded points represent individual samples.

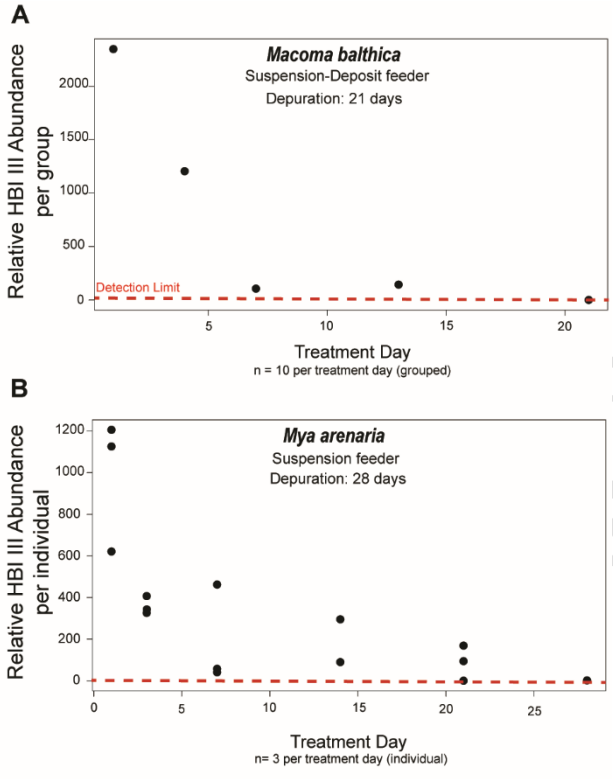

Figure 8 – Experimental HBI III depuration rates in temperate clam samples. (A) suspension-surface deposit feeding *Macoma balthica.* Individual points represent n=10 clams. (B) suspension feeding *Mya arenaria*. Individual points represent n=1 clam. The red-dashed line indicates the GC-MS detection limit for HBIs.